



OPEN Influence of physical shape and salting on tomato drying performance using mixed mode solar and open-air methods in semi-cloudy weather

Abdallah Elshawadfy Elwakeel^{1✉}, Guma Ali^{2,3✉}, Abdalla Zain Eldin⁴, Mohamed Mahmoud Alsebiey¹, Aml Abubakr Tantawy⁵, Mohammad S. AL-Harbi⁶, Atef Fathy Ahmed⁶ & Khaled A. Metwally⁷

SD Solar drying is increasingly recognized as a sustainable and energy-efficient solution for preserving agricultural products, offering a practical alternative to fossil fuel-dependent methods and traditional open sun drying (OSD). However, its overall performance is highly influenced by environmental variability and system design. This study provides a detailed evaluation of a newly developed direct solar dryer (DDSD) for tomato dehydration, conducted under real and fluctuating climatic conditions in Aswan, Egypt, from February 22 to 27, 2025. During the trial period, solar irradiance ranged widely from 88 to 826 W/m² due to intermittent cloud cover, while ambient temperatures fluctuated between 22 and 34 °C—conditions representative of actual field environments. Tomato samples were prepared in three physical forms—halves, quarters, and 6 mm slices—and subjected to two pretreatment methods (salted and unsalted) to assess their effects on drying kinetics. The DDSD demonstrated significantly better performance than OSD, reducing drying durations by 25–39.6%. The most efficient results were achieved for salted 6 mm slices, which dried in just 9 h—substantially faster than the 29 h for unsalted halves in DDSD and 48 h in OSD. These samples also exhibited the highest effective moisture diffusivity (D_{eff}) ($5.92 \times 10^{-9} \text{ m}^2/\text{s}$), reflecting enhanced internal moisture transport. Among 12 drying models evaluated, the Logistic model most accurately described the drying behavior in the DDSD, with an excellent statistical fit ($R^2 = 0.999524$, $\chi^2 = 6.74 \times 10^{-5}$, RMSE = 0.006868). Economically, the DDSD, integrated with a photovoltaic (PV) system, required a modest initial investment of \$520 and achieved a payback period of just 1.82 years for salted slices due to faster processing and increased throughput. From an environmental perspective, the system is projected to offset approximately 105.68 metric tons of CO₂ emissions over a 20-year lifespan, with an energy payback time of only 1.10 years and potential revenue of \$1321.04 from carbon credits. These findings underscore the DDSD's potential as a cost-effective, environmentally sustainable, and technically efficient solution for agricultural drying in solar-rich regions.

Keywords Tomato fruit, SD, Drying kinetics, Mathematical modeling, Thin layer modeling, Economic analysis, Environmental analysis

Abbreviations

¹Agricultural Engineering Department, Faculty of Agriculture and Natural Resources, Aswan University, Aswân 81528, Egypt. ²Department of Computer and Information Science, Faculty of Technoscience, Muni University, Arua, Uganda. ³Department of Computer Science and Engineering, Saveetha School of Engineering, Saveetha Institute of Medical and Technical Sciences, Chennai, Tamil Nadu, India. ⁴Agricultural and Biosystems Engineering Department, Faculty of Agriculture, Alexandria University, Alexandria, Egypt. ⁵Food Science Department, Faculty of Agriculture, Beni-Suef University, Beni-Suef 65211, Egypt. ⁶Department of Biology, College of Science, Taif University, P.O. Box 11099, 21944 Taif, Saudi Arabia. ⁷Soil and Water Sciences Department, Faculty of Technology and Development, Zagazig University, Zagazig 44519, Egypt. ✉email: abdallah_elshawadfy@agr.aswu.edu.eg; a.guma@muni.ac.ug

OSD	Open sun drying
DDSD	Developed direct SD
D_{eff}	Effective moisture diffusivity
PV	Photovoltaic
MC	Moisture content
DRs	Drying rates
PVT	Photovoltaic thermal
R^2	Coefficient of determination
RMSE	Root mean square error
χ^2	Chi-square
EPBT	Energy payback time
EE	Embodied energy
ECC	Emission carbon credit
k_D	Drying coefficient
MR_{exp}	Experimental moisture ratio
MR_{pre}	Predicted moisture ratio

List of symbols

M_d	Amount of tomato dried per batch
D_d	Drying time per batch
C_{ds}	Total cost of one kilogram
S_{kg}	Cost savings
S_1	Cost savings
m_{ev}	Total water removed
L	Half of slab thickness
n	Term number
W_w and W_d	Wet and dry weights
M_e	Equilibrium moisture content
M_0	Initial moisture content
M_t	Time-dependent moisture content
k_D	Drying coefficient
t	Time
A	Empirical correction factor
N	Number of observations
d	Interest rate
C_m	Maintenance cost
V_a	Salvage value
τ	Operating life
i	Inflation rate
D_d	Drying days per year
C_{fd}	Cost of fresh tomato
SP_c	Selling price of dried tomato
C_{ac}	Annual capital cost
C_{cc}	Total capital cost
F_c	Capital recovery factor
C_s	Drying cost per kg
D	Number of available drying days per year
	Latent heat of vaporization

Tomato (*Solanum lycopersicum*) is one of the most important horticultural crops cultivated worldwide, valued for its nutritional, economic, and industrial significance^{1–4}. It plays a central role in the human diet and is widely consumed in both fresh and processed forms, such as sauces, juices, pastes, and dried products. Tomatoes are rich in essential nutrients including vitamin C, vitamin A, potassium, and dietary fiber^{5,6}. Additionally, they are a major source of lycopene—an antioxidant compound that has been associated with reducing the risks of cancer and cardiovascular diseases⁷. Due to their health benefits and culinary versatility, tomatoes have become a dietary staple across cultures and a vital commodity in the global food supply chain⁸.

Globally, tomato production has grown steadily, reaching over 180 million metric tons in recent years, according to data from the Food and Agriculture Organization⁹. Major producers include China, which accounts for over 30% of global output, followed by India, the United States, Turkey, and Egypt. The widespread adaptability of tomato to various climatic conditions, short growing cycle, and high market demand have all contributed to its dominance among vegetable crops^{9–12}.

Egypt is one of the leading producers of tomatoes in the Middle East and North Africa region, ranking among the top ten producers globally. With annual production exceeding 6.5 million tons, tomatoes represent a major component of Egypt's vegetable production sector. They are cultivated year-round across several governorates including Beheira, Sharqia, Minya, and Aswan, benefiting from Egypt's diverse agro-climatic zones^{13,14}. Tomatoes in Egypt are mostly consumed locally in fresh form, but a growing portion is processed into products such as paste, juice, and dried tomatoes for both domestic use and export. Despite the large production volume, Egypt's tomato export levels remain modest^{15,16}. The amount of dried tomato production and export is particularly limited, representing a very small share of total output. Most dried tomatoes are produced in small-scale operations or traditional methods without standardized processing techniques or quality control

systems^{17,18}. As a result, the volume of dried tomatoes exported from Egypt remains below its potential, and international competitiveness is constrained by inconsistent product quality and limited compliance with export standards^{19,20}.

One of the main challenges hindering the development of Egypt's dried tomato industry is the widespread reliance on OSD. This traditional method involves placing tomato slices or halves directly under sunlight on rooftops or open fields²¹. While this method is low-cost and utilizes renewable energy, it is fraught with significant limitations. Chief among these is the risk of contamination by dust, insects, and other environmental pollutants, which raises serious food safety concerns^{22,23}. Moreover, sun drying is highly weather-dependent, with fluctuations in temperature, humidity, and solar radiation leading to inconsistent drying rates (DRs) and uneven moisture content (MC) across the product^{24,25}. Additionally, OSD often results in substantial losses of nutritional and sensory quality. Prolonged exposure to direct sunlight and high temperatures can degrade vital compounds such as vitamin C and lycopene^{26,27}. Furthermore, the extended drying periods required for complete dehydration increase the risk of microbial spoilage, especially under humid or cloudy conditions^{2–4,28,29}. The lack of proper hygiene, airflow control, and protection against rain or dew can further deteriorate product quality, making it unsuitable for high-value markets^{21,30–32}. In summary, tomatoes are a crop of strategic importance both globally and in Egypt, offering significant opportunities for value addition through drying and export. However, the full potential of Egypt's tomato industry—especially in dried tomato products—remains underutilized due to the limitations of OSD. Addressing these challenges through the adoption of improved drying technologies, such as solar dryers (SDs) or hybrid systems, could greatly enhance product quality, reduce post-harvest losses, and open new market avenues for Egyptian tomato producers.

Mathematical modeling of drying kinetics plays a crucial role in understanding, designing, and optimizing drying processes, particularly in food and agricultural engineering^{33,34}. Drying is a complex process influenced by factors such as temperature, air velocity, relative humidity, sample thickness, and the physical and chemical properties of the product. Through mathematical models, it becomes possible to predict MC removal behavior over time, and estimate DRs under different conditions^{35–37}. Modeling provides a scientific basis for simulating drying behavior without the need for extensive experimental trials, thus saving time and resources. It also helps in identifying the most appropriate drying conditions to preserve product quality, reduce energy consumption, and minimize nutritional losses^{38–40}. Various empirical, semi-theoretical, and theoretical models are used to describe drying kinetics, each offering unique advantages in terms of accuracy, simplicity, or applicability. In the context of drying food products like tomatoes, mathematical modeling is especially important to ensure uniform drying, maintain color and texture, and meet food safety standards^{14,41–43}. It also supports the development of advanced drying technologies such as solar or hybrid dryers. Overall, drying kinetics modeling is a vital tool in enhancing the efficiency, sustainability, and quality control of drying operations^{21,44,45}.

On the other hand, conducting an economic and environmental analysis of the SD is crucial for assessing the overall feasibility, cost-effectiveness, and long-term sustainability of drying systems, especially within the agro-industrial sector^{9,46}. Drying is a highly energy-intensive process, and optimizing it not only impacts product quality but also has significant economic and environmental implications^{28,47}. By analyzing drying kinetics, researchers and engineers can determine the most efficient operating conditions that minimize energy use, reduce drying time, and lower operational costs. Where economic analysis helps quantify the financial viability of drying technologies by assessing key parameters such as investment cost, payback period, energy consumption, and cost savings^{48,49}. It enables decision-makers to select systems that offer the best return on investment while maintaining product quality. Meanwhile, environmental analysis evaluates the ecological footprint of the drying process, focusing on energy efficiency, carbon emissions, and resource utilization^{50,51}.

Photovoltaic thermal (PVT) systems have emerged as a promising innovation in enhancing the efficiency of SDs. By integrating PV panels with thermal collectors, PVT systems simultaneously generate electricity and capture thermal energy, maximizing the utilization of solar radiation. This dual functionality addresses two major energy needs in solar drying: providing heat for moisture removal and supplying electricity for components such as fans or controllers. As a result, PVT-assisted SDs offer improved drying performance, reduced dependency on external power sources, and enhanced sustainability. Their application is particularly beneficial in agricultural settings, where efficient and eco-friendly drying methods are crucial^{52–55}.

SDs operate using natural convection, forced convection, or a combination of both in mixed-mode systems to remove moisture from agricultural products. Among these, forced air circulation dryers consistently outperform natural convection systems in terms of drying speed, energy efficiency, and product quality. They achieve higher collector and drying efficiencies—up to 77.2% and 12.11%, respectively—compared to natural convection dryers, which may reach as low as 56.84% and 6.62%^{56–59}. Forced convection also enables faster and more uniform moisture removal, leading to reduced drying times and improved final product characteristics^{58–61}. Additionally, they demonstrate lower specific energy consumption and higher moisture extraction rates, making them particularly efficient for high-moisture content crops^{56,58,59,61}. On the other hand, mixed-mode SDs, which alternate between forced and natural convection depending on solar availability, offer a flexible and energy-optimized solution. During peak sunlight, forced convection ensures performance, while at night or under low radiation, the system switches to natural convection, reducing energy demand^{62,63}. These systems also show higher CO₂ mitigation potential^{57,62,63}, better sustainability indices, and improved economic feasibility, often reducing payback periods by using fans only when necessary^{62,63}. While natural convection dryers are simpler and more cost-effective—ideal for rural, off-grid settings—they generally deliver lower performance⁶⁴. Forced convection systems, despite their higher initial cost and energy needs (often met via solar photovoltaic panels), offer significantly better drying outcomes^{56–59}. Thus, mixed-mode dryers represent an optimal balance, combining the efficiency of forced airflow with the simplicity and sustainability of natural drying^{62,63}. Their adaptability to fluctuating weather and power conditions makes them highly suitable for sustainable, high-quality food preservation, especially in regions with variable solar resources.

The novelty of this study lies in the development of a direct SD integrated with an intelligent, temperature-responsive control algorithm capable of dynamically switching between natural and forced convection based on real-time temperature data. Unlike previous systems with fixed or manually operated airflow mechanisms, this adaptive design significantly improves drying efficiency, reduces energy consumption, and minimizes the risk of over-drying or product spoilage. The implementation of a fully automated, solar-powered control system within a cost-effective structure presents a scalable and sustainable solution, particularly suited for off-grid agricultural communities. Furthermore, this study uniquely combines drying kinetics modeling with comprehensive economic and environmental evaluations to provide a holistic understanding of system performance. Such an integrated approach aligns with global sustainability goals by supporting renewable energy use and reducing greenhouse gas emissions. In sun-rich regions like Egypt, this work offers practical advancements in eco-friendly tomato drying. The study also investigates the effects of physical shape and salting on drying behavior under semi-cloudy sky conditions.

Materials and methods

Description of the DDSD

To achieve the objectives of this study, a DDSD was purposefully designed and constructed. The layout and key components of the DDSD are illustrated in Fig. 1. The DDSD integrates multiple functional elements that work together to optimize its performance and drying efficiency. These include: (1) three DC fans for air intake, (2) a main drying chamber loaded with tomato samples, (3) a transparent glass cover for solar transmission, (4) an IoT-based sensing and data logging unit, (5) a voltage regulator, (6) two DC exhaust fans for air discharge, (7) a durable metallic support frame, (8) a 100-W PV solar panel, (9) six drying trays, and (10) a laptop for monitoring and data collection. The dryer measures 300 cm in length, 100 cm in width, and 20 cm in depth. Its top is sealed with a 3 mm thick glass sheet that facilitates solar energy absorption while minimizing thermal losses. The DDSD's base features a corrugated black aluminum absorber plate, chosen for its high solar absorption efficiency, and insulated with a 3 cm thick layer of mineral wool to enhance heat retention. Inside the chamber, six trays (each 100 cm × 50 cm) hold the drying material. For effective ventilation and uniform drying, five 12 V DC brushless fans (0.20 A) are installed—three as air inlets and two as exhaust outlets to expel moist air. This setup ensures balanced airflow and consistent moisture removal across all drying layers. The system also incorporates a smart monitoring solution powered by IoT technology. A DHT-22 sensor measures internal and external air temperature and relative humidity in real-time. These values are managed via an Arduino Uno microcontroller and stored using a micro-SD card module for subsequent data analysis. The DDSD operates independently using a 100 W PV solar panel connected to a voltage converter (12 V to 5 V), making it fully off-grid and energy-efficient. Figure 1 offers a detailed visual layout of the DDSD and its interconnected components. Figure 2 shows the position of DHT sensors within the DDSD and control circuit. Table 1 shows the accuracy, range, and error of the measuring devices and sensors. And Fig. 3 presents the technical specification of the PV system for the current study.

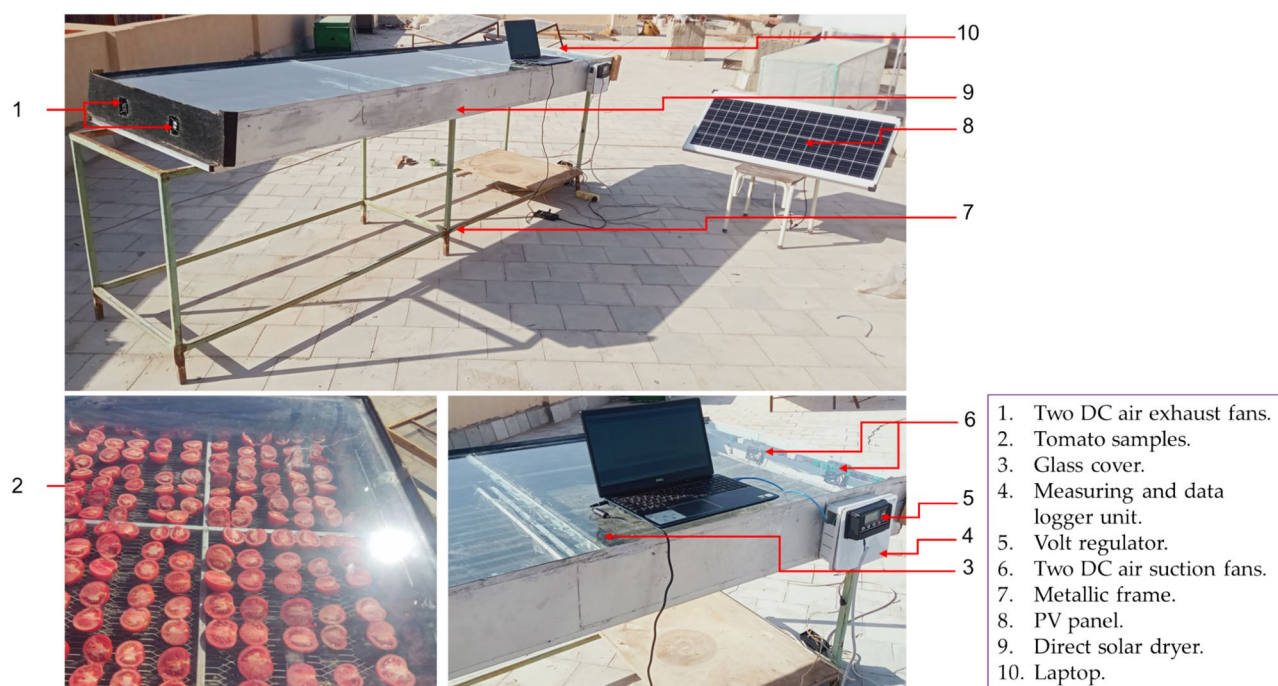


Fig. 1. Main components of the DDSD.

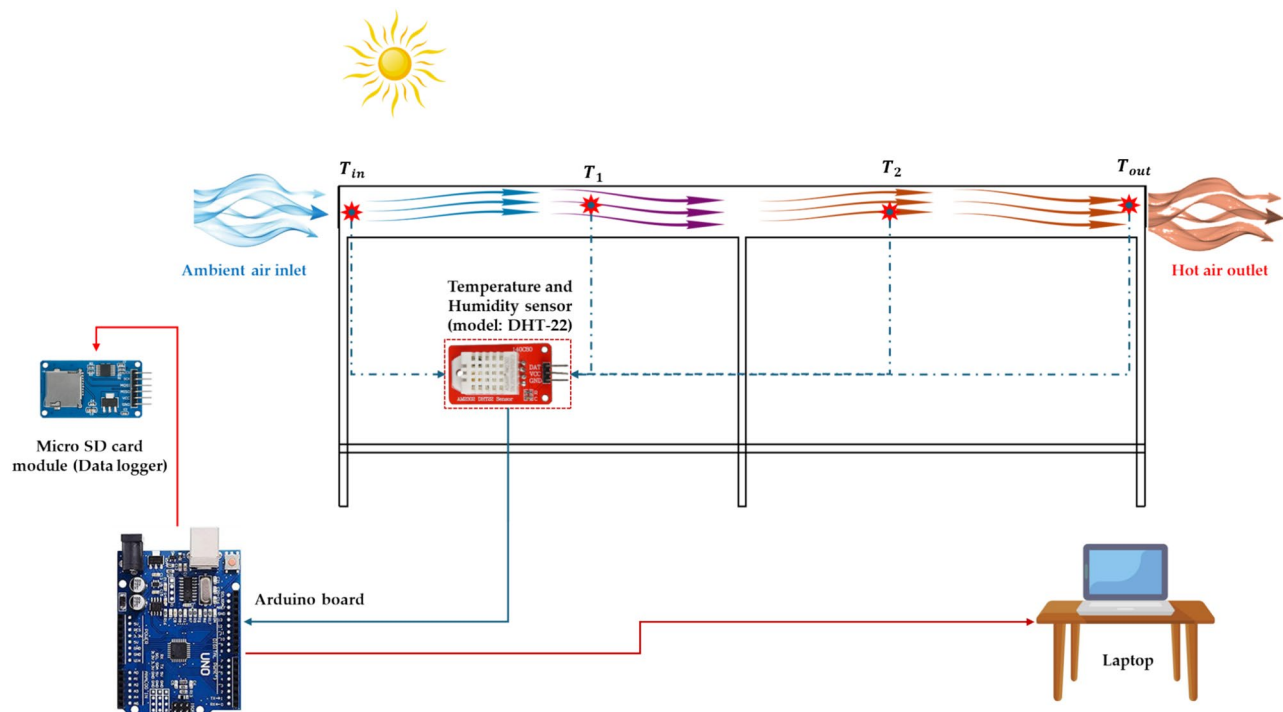


Fig. 2. Schematic diagram showing the position of DHT sensors within the DDSD and control circuit.

Parameters	Device	Precision	Range	Error
Air temperature	DHT-22 sensor	$\pm 1\text{ }^{\circ}\text{C}$	$-10\text{--}80\text{ }^{\circ}\text{C}$	$0.1\text{ }^{\circ}\text{C}$
Relative humidity	DHT-22 sensor	$\pm 2\%$	0–100%	0.1%
Solar radiation	Spectral pyranometers (model: _SENTEC RS485, Sichuan, China)	$\pm 10\text{ W/m}^2$	–	0.1 W/m^2
Weight of samples	Electronic digital balance	$\pm 0.020\text{ g}$	0.0–50 kg	5 g
Voltage and current (PV system)	Digital multi-meter	–	0.2–1000 V 20 μA –20 A	0.01 V 0.01 A
Air speed	Digital anemometer (model: Extech AN100, China)	$\pm 0.1\text{ m/s}$	0.0–30 m/s	0.1 m/s
Light intensity	LDR sensor	$\pm 1\text{ Lux}$	0.0–1000 Lux	0.1 Lux

Table 1. The precision, measurement range, and error margins of the sensors and instruments.

Operational algorithm for the DDSD

The operational algorithm for the DDSD is illustrated in Fig. 4. The process begins with the initialization of temperature sensors, followed by the real-time collection of temperature data from multiple sensor points within the system. The algorithm then evaluates whether the recorded air temperature exceeds a predefined threshold (Set Point = $40 \pm 2\text{ }^{\circ}\text{C}$).

- I. If the temperature remains within the acceptable range, the system operates under natural convection, allowing ambient airflow to facilitate the drying process.
- II. If the temperature exceeds the set point, the algorithm automatically activates forced convection by powering the air circulation fans to enhance heat and moisture transfer.

This adaptive airflow control mechanism ensures that the appropriate air circulation mode—natural or forced—is selected dynamically based on the current drying conditions. After the airflow mode is determined, the algorithm imposes a 5-min delay before repeating the monitoring cycle to maintain system stability and prevent frequent switching.

The primary aim of this algorithm is to optimize the drying process by continuously adjusting air circulation in response to real-time temperature data. This intelligent control strategy not only enhances drying efficiency, but also helps prevent over-drying and minimize product spoilage. Furthermore, by relying solely on solar energy and automatically regulating airflow, the DDSD offers a sustainable and energy-efficient alternative to conventional dryers that typically depend on fossil fuels.

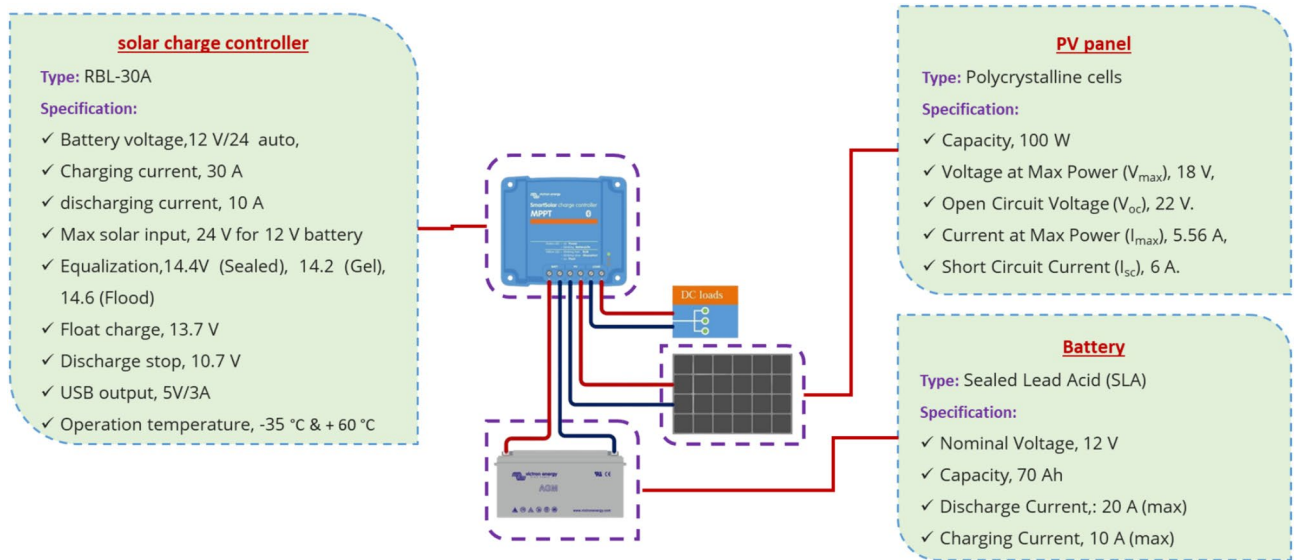


Fig. 3. The PV system's technical specifications used in this study.

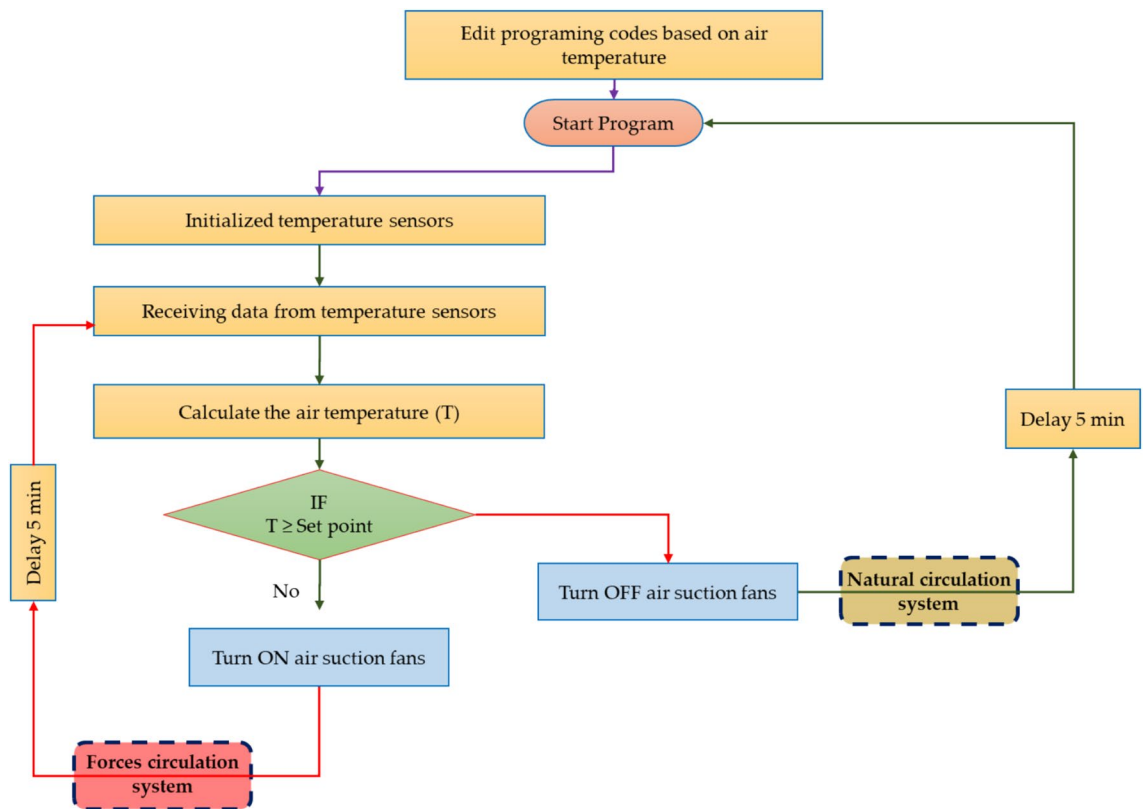


Fig. 4. Operating algorithm of the DDS.

Experiment design

The drying experiments were conducted daily from 8:00 a.m. to 5:00 p.m. in the Faculty of Agriculture, Aswan University, from February 22 to 27, 2025. The main aim was to assess and contrast the efficacy of two solar drying techniques: the DSD and the OSD. Fresh tomatoes obtained from a local market in Aswan, Egypt, constituted the testing material. The initial MC of these tomatoes was around 92.5% (w.b.), consistent with values documented in prior research^{14,17–20,65}. Before the drying process, the tomatoes were meticulously cleaned with tap water to remove any surface impurities (Fig. 5). Following washing, surplus water was meticulously eliminated, and the

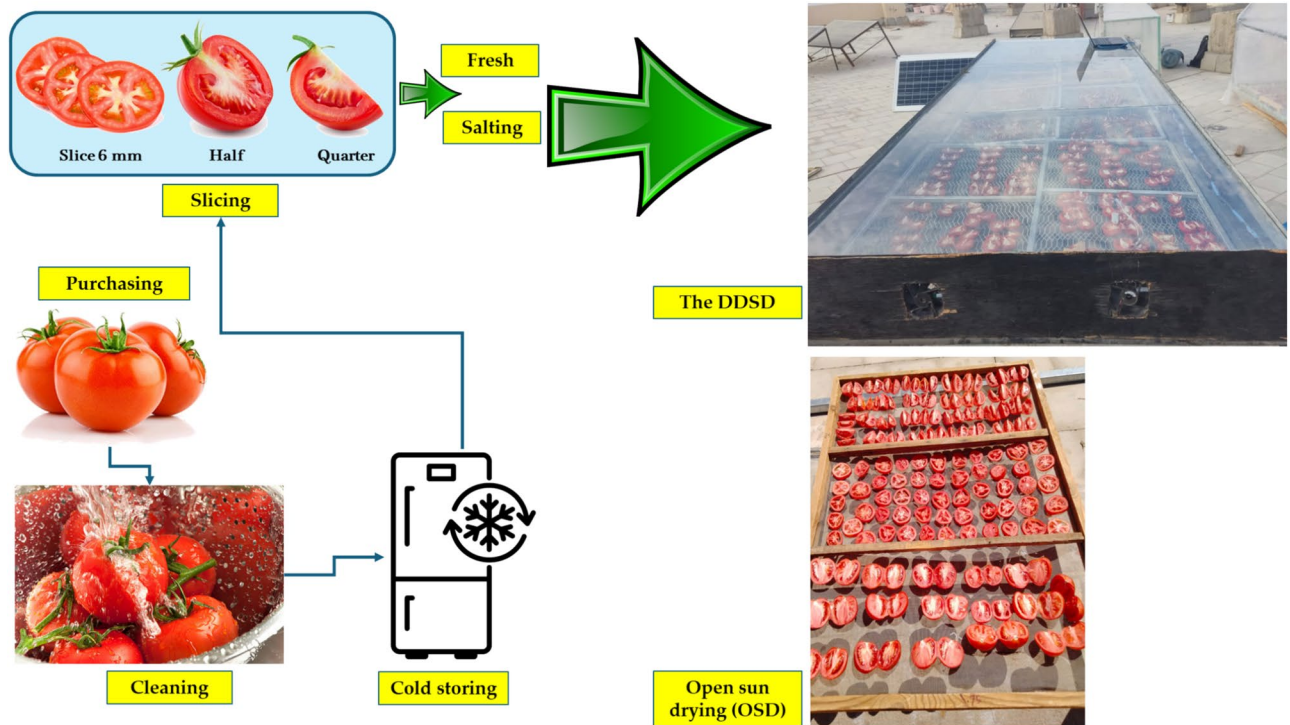


Fig. 5. Preparation steps for drying tomato samples.

tomatoes were cut into different physical shapes, including 6 mm slices, quarters, and half. Subsequent to the preliminary preparation, the tomato samples were uniformly arranged in a single layer over the drying trays to guarantee consistent airflow exposure. The samples were rigorously allocated into two experimental groups for comparative analysis. The first tomato samples were subjected to a surface treatment with food-grade sodium chloride (NaCl, purity $\geq 99.5\%$), applied uniformly at a concentration of 2% w/w. The remaining tomato samples were left unsalted to establish a baseline for assessing the impact of salt application on drying kinetics. This binary experimental design enabled direct comparison between salted and unsalted samples under uniform drying circumstances, hence easing the evaluation of salt's impact on D_{eff} . During the drying trials, several critical parameters were systematically observed and documented hourly. During the study period the average solar radiation, ambient temperature, and wind speed were ranged between (88 and 826 W/m²), (22 and 3 °C), and (0 and 0.2 m/s).

Performance analysis

Moisture content (MC)

The determination of MC for fresh tomato was estimated in a laboratory electric oven set at a constant temperature of 70 °C until reaching the constant weight. Then, the MC was calculated using Eqs. 1 and 2⁶⁶.

$$MC (d.b.) = \frac{W_w - W_d}{W_d} \times 100 \quad (1)$$

$$MC (w.b.) = \frac{W_w - W_d}{W_w} \times 100 \quad (2)$$

where, W_w and W_d are the wet and dry weights of tomato sample, respectively, in g.

Moisture ratio (MR)

Equation 3, as referenced in⁶⁷, is utilized to calculate the MR during the drying process. This equation serves as a fundamental tool in drying kinetics analysis, offering a reliable and precise method for quantifying the rate at which moisture is removed from the product over time. Accurate determination of MR is critical for assessing the efficiency of the drying system, comparing different drying methods, and modeling the moisture removal behavior under varying conditions. By tracking the reduction in MC relative to the initial and equilibrium MC, the MR provides a dimensionless parameter that facilitates standardization and comparison across diverse experimental setups. The consistent application of Eq. 3 enables a thorough interpretation of drying curves and supports the validation of mathematical models used to simulate drying kinetics, thereby contributing significantly to the overall evaluation and optimization of the drying process.

$$MR = \frac{M_t - M_e}{M_0 - M_e} \quad (3)$$

The drying kinetics of tomato samples represent a key area of scientific investigation, commonly analyzed using the MR in conjunction with appropriate mathematical modeling. In this context, it has been established that the equilibrium MC (M_e) is significantly lower than both the initial (M_0) and time-dependent MC (M_t), making its influence negligible in most practical scenarios. Consequently, the MR can be simplified by excluding M_e , leading to a more streamlined expression of the drying behavior. This simplified form of MR, applicable to tomato drying, is presented in Eq. 4, as referenced in⁴³, and is widely adopted for modeling and comparative analysis of drying processes.

$$MR = \frac{M}{M_0} \quad (4)$$

Drying constant (k)

The drying constant (Eq. 5), also referred to as the drying coefficient, is a fundamental parameter in characterizing thin-layer drying behavior. It is influenced by a combination of transport properties, including mass transfer coefficients, material density, specific heat capacity, D_{eff} , thermal conductivity, and interfacial heat transfer⁴³. This constant is typically derived from the exponential correlation between the MR and drying time, which serves as a standard model for evaluating drying kinetics. Although the drying constant plays a critical role in describing and predicting the drying kinetics of agricultural materials^{33,43}, it is essential to recognize that it encapsulates the effects of multiple coupled transport phenomena. Accurate interpretation therefore requires careful consideration of the interactions between thermal and mass transfer mechanisms that govern moisture migration during the drying process.

$$\frac{dM}{dt} = -k_D \times (M - M_e) \quad (5)$$

The solution to Eq. 5 is obtained through the integration of Eq. 6^{33,43},

$$MR = \frac{M_t - M_e}{M_0 - M_e} = \exp(-k_D \times t) \quad (6)$$

Drying rate (DR)

The DR is calculated using Eq. 7³³. This equation is widely recognized and accepted in both academic research and industrial applications for its accuracy and reliability in quantifying moisture removal over time. Its consistent use across numerous studies ensures the generation of precise, reproducible results—an essential requirement in scientific experimentation. By applying this established methodology, researchers can effectively evaluate and compare drying performance under various operational conditions, contributing to the robustness and validity of drying kinetics analyses.

$$DR = \frac{M_t - M_{(t+dt)}}{dt} \quad (7)$$

Moisture diffusivity (D_{eff})

Fick's second law of diffusion, represented mathematically in Eq. 8, has been utilized to examine the drying process, specifically focusing on the removal of moisture from materials²⁵. This law serves as a cornerstone in diffusion theory, providing a quantitative description of how the concentration of a substance—such as water vapor—changes with time within a given medium due to molecular diffusion. In the context of drying, it models the time-dependent movement of moisture from the interior of a material to its surface, where it eventually evaporates. By applying Fick's second law, researchers are able to predict the rate at which moisture is eliminated, offering critical insights into the drying kinetics and overall behavior of the material under varying drying conditions. This theoretical approach enables the optimization of drying parameters to enhance efficiency, product quality, and energy usage in industrial and laboratory-scale drying operations.

$$\frac{\partial M}{\partial t} = D_{eff} \times \nabla^2 M \quad (8)$$

The drying behavior of food and agricultural products, particularly during the falling rate period, can be effectively described using Fick's second law of diffusion. This stage of drying is predominantly governed by internal moisture migration rather than surface evaporation. To quantify this moisture movement, Eq. 8 is employed, which was originally developed in⁶⁸ for an idealized case involving an infinite slab geometry. This model operates under several simplifying assumptions: moisture transport occurs in a single direction (unidimensional), the temperature remains constant throughout the process, the material undergoes no significant volumetric changes, the D_{eff} is uniform, and external resistance to mass transfer is minimal. These assumptions help streamline the complex physical phenomena into a mathematically tractable form. It is important to highlight that this equation has been widely adopted and validated in various studies^{18,19,68}, reinforcing its relevance and reliability in modeling the drying kinetics of diverse agricultural and food-based materials.

$$MR = \frac{M_t}{M_0} = \frac{8}{\pi^2} \times \sum_{n=1}^{\infty} \frac{1}{n^2} \exp\left(\frac{-\pi^2 \times D_{eff} \times t}{4L^2}\right) \tag{9}$$

where: M_0 is the initial MC; n is the term number; t is the time in s; L is the half of slice thickness (m).

By omitting the higher-order terms in Eq. 9—terms that primarily influence the model at extended drying times—a simplified form can be derived to estimate the D_{eff} of tomato, as shown in Eq. 10. This approximation is achieved by retaining only the first term of the series expansion, while disregarding the remaining terms, which have a negligible effect during the early and intermediate stages of drying.

$$MR = \frac{8}{\pi^2} \times A \exp\left(\frac{-\pi^2 \times D_{eff} \times t}{4L^2}\right) \tag{10}$$

Equation 11 has been obtained mathematically by taking the natural logarithm on both sides of Eq. 10.

$$\ln(MR) = \ln\left(\frac{8}{\pi^2}\right) - \left(\frac{\pi^2 \times D_{eff} \times t}{4L^2}\right) \tag{11}$$

The D_{eff} is obtained by plotting experimental drying data in terms of $\ln(MR)$ versus time, s.

Mathematical modelling of tomato drying

Twelve thin-layer models, listed in Table 2, were employed to interpret and evaluate the experimental data collected during the drying process. Each set of experimental results obtained from different drying techniques was fitted to these models in order to analyze drying behavior accurately. Non-linear regression analysis was performed using OriginLab and Microsoft Excel software to determine the model coefficients and associated statistical parameters. This approach of curve fitting is widely used across various scientific disciplines, particularly in biology, to translate complex experimental observations into standardized mathematical expressions. Curve fitting serves as a powerful tool to mathematically represent experimental data, allowing for more consistent interpretation and comparison. The quality of a model's fit indicates how closely the mathematical function represents the observed data—the better the fit, the more reliable and predictive the model.

To identify the most suitable drying model, statistical indicators such as the coefficient of determination (R^2), root mean square error (RMSE), and chi-square (χ^2) were used. The optimal model was determined based on the highest R^2 value, indicating a strong correlation with experimental data, and the lowest values of RMSE and χ^2 , reflecting minimal deviation between predicted and observed values^{34,69,70}.

These parameters can be calculated using the following Eqs. 12–14^{71–73},

$$RMSE = \sqrt{\frac{1}{N} \sum_{i=1}^N (MR_{pre,i} - MR_{exp,i})^2} \tag{12}$$

No	Model	Model equation
1	Newton (Lewis)	$MR = \exp(-kt)$
2	Page	$MR = \exp(-kt^n)$
3	Simplified Fick's diffusion	$MR = a \exp\left(-c\left(\frac{t}{L^2}\right)\right)$
4	Approximation or diffusion or diffusion approach	$MR = a \exp(-kt) + (1 - a) \exp(-kbt)$
5	Combined two-term and page	$MR = a \exp(-kt^n) + b \exp(-ht^n)$
6	Modified Henderson and Pabis	$MR = a \exp(-kt) + b \exp(-gt) + c \exp(-ht)$
7	Modified Midilli II	$MR = a \exp(-kt^n) + b$
8	Modified Page III	$MR = k \exp\left(-\frac{t}{d^2}\right)^n$
9	Modified two term III	$MR = a \exp(-kt) + (1 - a) \exp(-kat)$
10	Logistics	$MR = \frac{b}{1 + a \exp(kt)}$
11	Logarithmic (asymptotic)	$MR = a \exp(-kt) + c$
12	Parabolic model	$MR = a + bt + ct^2$

Table 2. Mathematical models that explain the drying curve for tomatoes fruits at OSD and DDSD^{33,43,67}..

* MR is the moisture ratio; k , is the drying constants, h^{-1} ; t is the drying time, h ; a , b , c , d , g , h , n are the model constants, dimensionless; L is the half of slab thickness, m

$$\chi^2 = \frac{\sum_{i=1}^N (MR_{pre,i} - MR_{exp,i})^2}{N - n} \quad (13)$$

$$R^2 = 1 - \frac{\sum_{i=1}^N (MR_{pre,i} - MR_{exp,i})^2}{\sum_{i=1}^N (\overline{MR}_{pre} - MR_{exp,i})^2} \quad (14)$$

where: $MR_{exp,i}$ and $MR_{pre,i}$ are the i th experimental and predicted values; \overline{MR}_{pre} is the average predicted values; N is the number of observations; n is the number of constants in a model.

Economic analysis

A detailed economic evaluation was carried out to assess the financial feasibility of the DSDDSD, with a particular focus on its viability within the economic framework of Egypt. This analysis was grounded in widely recognized methodologies for assessing renewable energy technologies^{74–76}, ensuring consistency and reliability in the evaluation process. Three critical economic performance indicators were examined: (1) the annualized investment cost (C_a), which reflects the distribution of capital costs over the system's lifespan; (2) the payback period (N), representing the time required to recover the initial investment; and (3) the net cost saving value (S_j), indicating the economic benefit derived from operating the system over time. These indicators offer a comprehensive basis for evaluating the long-term commercial potential and return on investment of the SD. The annualized investment cost (C_a) for the developed DSD was computed using the financial equations provided in Eqs. 15–17⁷⁶, incorporating local economic parameters such as interest rates, equipment lifespan, and market pricing. This analytical approach ensures an accurate projection of the system's economic sustainability under real-world operating conditions. Table 3 shows the calculation assumptions of economic analysis of the DDSD based on economic aspects in Egypt.

$$C_a = C_{ac} + C_m - V_a \quad (15)$$

$$C_{ac} = C_{cc} \times F_c \quad (16)$$

$$F_c = \frac{d(1+d)^n}{(1+d)^n - 1} \quad (17)$$

where C_{ac} is the annual capital cost, n is the working life (20 years), and C_{cc} is the total capital cost, and F_c is the capital recovery factor.

The drying cost per kg of tomato fruit (C_s) using the DDSD (C_s) was calculated using Eq. 18^{74–76}.

$$C_s = \frac{C_a \times D_d}{M_d \times D} \quad (18)$$

where D is the number of available drying days per year, M_d is the amount of tomato dried per batch, and D_d is the drying time per batch.

The total cost of one kilogram of the dried tomato (C_{ds}) using the DDSD, was estimated using Eq. 19^{74–76}.

$$C_{ds} = C_{fd} \times \frac{M_f}{M_d} + C_s \quad (19)$$

where $\frac{M_f}{M_d}$ is the ratio between fresh and dried tomato per batch.

The cost savings per one kilogram of dried tomato (S_{kg}) was estimated using Eq. 20.

$$S_{kg} = SP_c - C_{ds} \quad (20)$$

where, SP_c is the selling price of dried tomato per kilogram.

Parameter	Nomenclature	Unit	Value
Interest rate	d	%	3
Maintenance cost	C_m	USD/year	3% of the annual capital cost
Salvage value	V_a	%	8% of the annual capital cost
Operating life	τ	year	20 years
Inflation rate		%	13.9
Drying days per year	D_d	day	350
Cost of fresh tomato	C_{fd}	USD/kg	0.2
Selling price of dried tomato	SP_c	USD/kg	2

Table 3. Calculation assumptions of economic analysis of the DDSD based on economic aspects in Egypt.

The cost savings (S_j) from the DDS For the DDS, the highest DR was recorded for salted tomato halv following (j) years were obtained by Eq. 21.

$$S_j = \frac{S_{kg} \times M_d}{D} \times D \times (1 + j)^{j-1} \quad (21)$$

The payback time (T_p) of the investigation cost was obtained using Eq. 22⁷⁴⁻⁷⁷.

$$T_p = \frac{\ln \left[1 - \frac{C_{cc}}{S_1} (d - i) \right]}{\ln \left(\frac{1+i}{1+d} \right)} \quad (22)$$

where, i is the inflation rate and S_1 is the cost savings after the first year.

Environment analysis

Embodied energy (EE)

The term embodied energy refers to the total amount of energy consumed during the manufacturing of both the DDS and the PV system. This includes all direct and indirect energy inputs associated with the extraction of raw materials, processing, transportation, and assembly of each component involved in constructing the DDS and PV system. To determine the EE, every stage of the manufacturing process is considered, allowing for a comprehensive evaluation of the system's energy footprint. The estimation of the embodied energy for both the DDS and PV system was performed using Eq. (23)⁷⁸. This equation enables the calculation of embodied energy by quantifying the cumulative energy demand based on the material and energy inputs. The resulting EE values offer insight into the sustainability and environmental impact of the systems. The calculated EE values for the ADS and PV system are presented in Table 4, providing a detailed comparison of the energy investments required for each component. This evaluation is essential for assessing the overall efficiency and lifecycle performance of the solar drying system.

$$EE = \text{Coefficient of embodied energy} \times \text{product weight} \quad (23)$$

Energy payback time (EPBT)

The EPBT of the DDS and the PV system were calculated using Eq. 24. This important metric represents the duration required for the system to recover, through its operation, the total amount of energy initially invested in its manufacturing, transportation, and installation processes. In other words, EPBT indicates how long the ADS and PV system must function to produce an equivalent amount of useful energy to offset the embodied energy consumed during their development. A shorter EPBT signifies a more energy-efficient and environmentally sustainable system, as it quickly compensates for the initial energy expenditure and begins contributing to net energy savings. This concept is crucial in evaluating the long-term viability and sustainability of renewable energy technologies. The methodology and rationale for EPBT estimation are based on principles outlined in references^{79,82}.

$$EPBT = \frac{EE}{\text{Annual energy output}} \quad (24)$$

where annual energy output from the DDS can be calculated using Eq. 25^{83,84}:

$$\text{Annual energy output} = \frac{m_{ev} \times l}{3.6 \times 10^6} \times \text{Operating days/year} \quad (25)$$

where, m_{ev} is the total water removed from tomato samples, l is the latent heat of vaporization.

No	Materials	Coefficient of embodied energy (kW h)	Weight	Embodied energy (kW h)	References
1	Metal frame	55.28 (kW h/kg)	20.0 (kg)	1105.6	79,80
2	Glass cover	7.28 (kW h/kg)	10 (kg)	72.8	81
3	Wood dust	2.0 (kW h/kg)	2.0 (kg)	4.0	
4	Paint	25.11 (kW h/kg)	1.0 (kg)	25.11	
5	Absorber plate	9.636 (kW h/kg)	10.5 (kg)	101.18	79,80
6	Air circulation fans	19.39 (kW h/kg)	0.5 (kg)	9.695	
7	PV system	1130.6 kW h/m ²	0.5 m ²	565.3	79,80
8	Battery	148.4515	-	46.00	
9	Battery charger	-	-	33.00	
Total embodied energy					1962.685 kWh

Table 4. Embodied energy calculation data for DDS integrated with PV system.

Carbon dioxide (CO₂) emissions

To estimate the annual carbon dioxide (CO₂) emissions associated with the operation of the DDS, it is essential to consider the source of the electrical energy it consumes. If the DDS relies on electricity generated from coal-fired power plants, the corresponding environmental impact can be quantified based on established emission factors. Typically, coal-based electricity production is associated with an emission factor of approximately 0.98 kg of CO₂ per kilowatt-hour (kg/kWh), as reported in previous studies^{79,85}. Using this emission factor, the total annual CO₂ emissions from the DDS can be calculated by applying Eq. 26, which accounts for the system's yearly energy consumption and translates it into its carbon footprint.

$$CO_2 \text{ emission per year} = \frac{EE \times 0.98}{Lifetime} \quad (26)$$

Equation 25 has been further refined and extended into Eq. 27 by incorporating additional real-world factors that influence the actual energy usage and related emissions. Specifically, this includes the losses incurred during the transmission and distribution of electricity—denoted as (L_{td})—as well as the losses associated with the operation of domestic appliances, represented by (L_{da}). These losses are particularly relevant when the electricity is sourced from coal-based power generation, which is known for its significant environmental impact. By accounting for these inefficiencies, Eq. 26 provides a more accurate and comprehensive assessment of the total energy demand and corresponding CO₂ emissions, ensuring that the calculation reflects practical conditions more realistically⁸⁶.

$$\text{The } CO_2 \text{ emission per year} = \frac{1}{1 - L_{da}} \times \frac{1}{1 - L_{td}} \times \frac{EE \times 0.98}{Lifetime} \quad (27)$$

Equation 28 is generated from Eq. 27 by assuming the values of L_{td} and L_{da} as 0.4 and 0.2, respectively^{76,87}.

$$\text{The } CO_2 \text{ emission per year} = \frac{EE}{Lifetime} \times 2.042 \text{ kg} \quad (28)$$

Net CO₂ mitigation and emission carbon credit (ECC)

The net CO₂ mitigation per lifetime of the DDS and PV system can be estimated using Eq. 29⁸³.

$$\text{Net } CO_2 \text{ mitigation per life time} = [\text{Annual energy output} \times \text{Lifetime} - EE] \times 2.042 \text{ kg} \quad (29)$$

The ECC represents the avoidance of one metric ton (1,000 kg) of CO₂ emissions. The carbon credit earned from the operation of the DDS was calculated using Eq. 30⁷⁸.

$$ECC = \text{Net mitigation of } CO_2 \text{ in life time} \times \text{Price per ton of } CO_2 \text{ mitigation} \quad (30)$$

Uncertainty analysis

The uncertainties associated with the measuring instruments were estimated using Eq. 31⁸¹. The initial uncertainty in determining MC, MR, and DR was calculated to be approximately 1.12%. Additionally, measurement errors for temperature, relative humidity, wind speed, and solar radiation were found to be 0.32%, 0.28%, 0.24%, and 0.13%, respectively. Taking all these variables into account, the overall uncertainty in evaluating the efficiency of the SD was estimated at around ±2%.

$$W_r = \left[\left(\frac{\partial R}{\partial x_1} W_1 \right)^2 + \left(\frac{\partial R}{\partial x_2} W_2 \right)^2 + \dots + \left(\frac{\partial R}{\partial x_3} W_3 \right)^2 \right]^{1/2} \quad (31)$$

Results and discussion

Weather conditions

In this study, a series of systematic experiments were carried out to assess the efficiency of a direct SD in dehydrating tomatoes under varying environmental and operational conditions. The trials were conducted between February 22 and 27, 2025, at the Faculty of Agriculture, Aswan University. The experiments were conducted daily from 8:00 AM to 5:00 PM, totaling 10 h of drying per day. In the graphical representations, the numbers from 1 onward denote the sequential order of the drying days, each representing a 10-h drying session. During the experimental period, the region was affected by a low-pressure weather system that brought unseasonably cool temperatures and intermittent cloud cover. These meteorological changes introduced considerable variability in solar irradiance and thermal conditions, posing challenges for consistent drying performance. As depicted in Fig. 6, solar radiation levels fluctuated notably throughout the day, particularly in the afternoon, decreasing from a high of 826 W/m² to 390 W/m². Daily solar irradiance showed a more pronounced decline, dropping from a peak of 826 W/m² to as low as 88 W/m² during periods of cloud cover. Meanwhile, ambient temperatures exhibited more stability, ranging from 22 °C in the early morning to a maximum of 31 °C by midday. Simultaneous monitoring of the dryer's thermal behavior indicated that internal temperatures ranged between 23.5 and 33 °C, while external temperatures showed a broader fluctuation, from 23 to 44.5 °C. These variations reflect the system's capacity to absorb and enhance ambient heat. On average, the air temperature inside the dryer surpassed the ambient temperature by approximately 0.5–12.5 °C, demonstrating the unit's ability to utilize solar energy effectively, even under suboptimal atmospheric conditions.

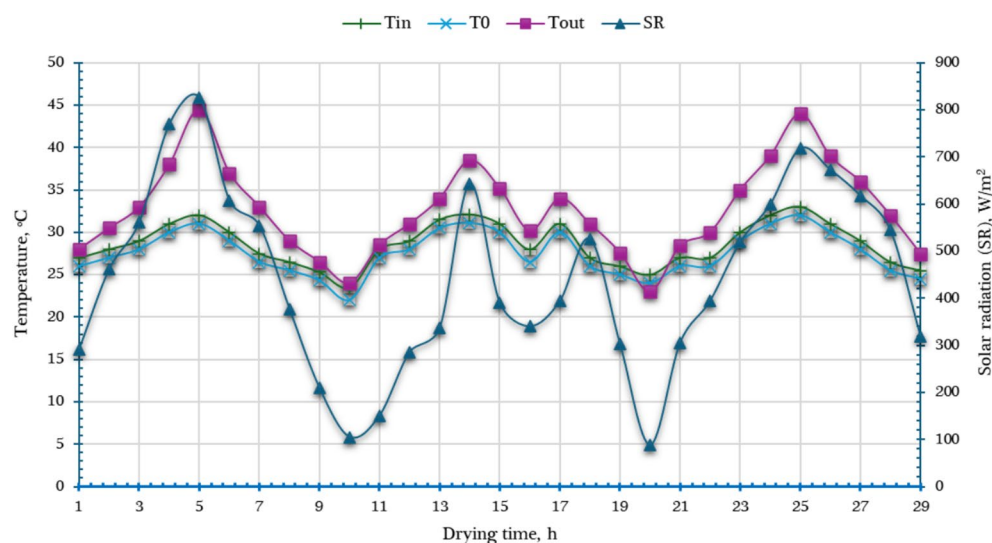


Fig. 6. Solar radiation (SR), ambient temperature (T_0), and inlet/outlet temperatures of the DDSD (T_{in} and T_{out}).

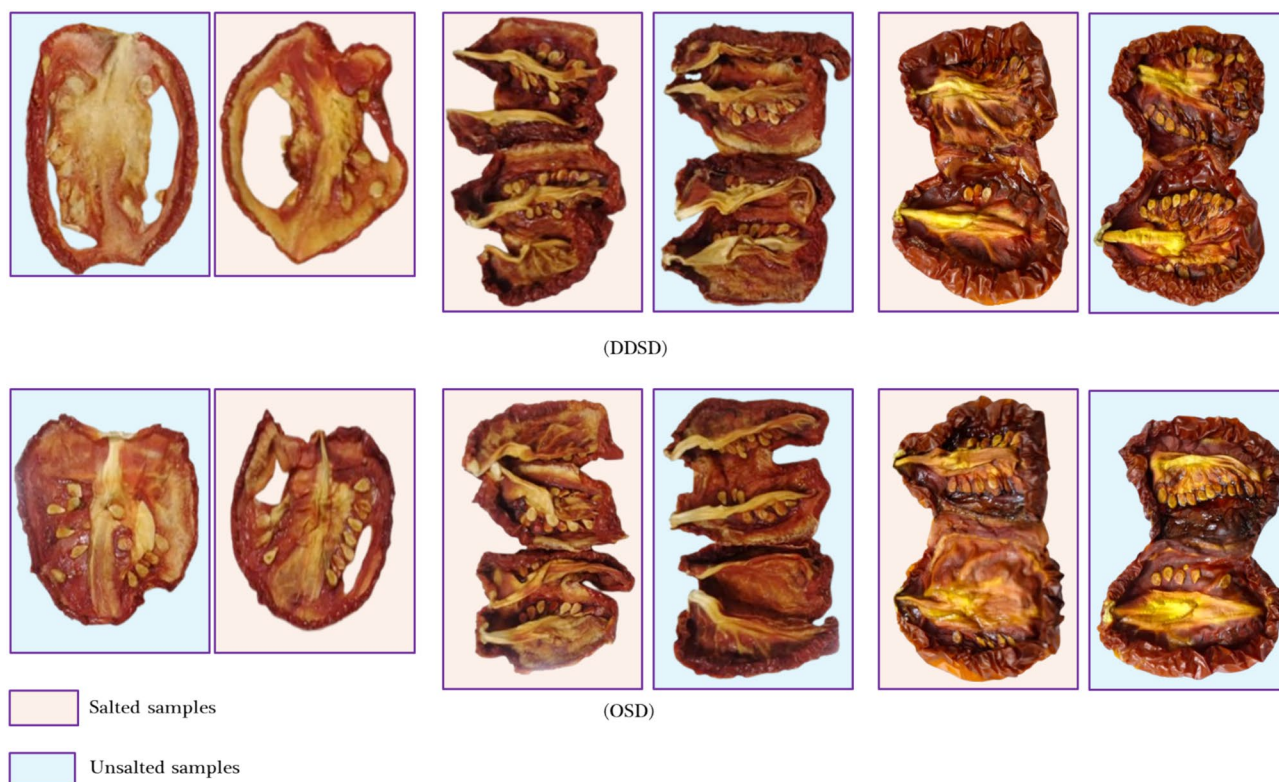


Fig. 7. Dried tomato samples.

Drying kinetics

To assess the drying performance of the DDSD, tomatoes were selected as the test biological material. The tomatoes were prepared in three distinct physical shapes—halves, quarters, and 6 mm thick slices—and subjected to two salting conditions: salted and unsalted. The initial MC of the fresh tomatoes was approximately 92.5% (w.b.), aligning with values reported in earlier studies^{88,89}. Figure 7 shows the final dried tomato samples using both drying systems.

Figure 8 illustrates the MC variations in the tomato samples dried using both the DDSD and a traditional OSD method. The drying period required to achieve equilibrium MC ranged from 12 to 48 h under OSD conditions.

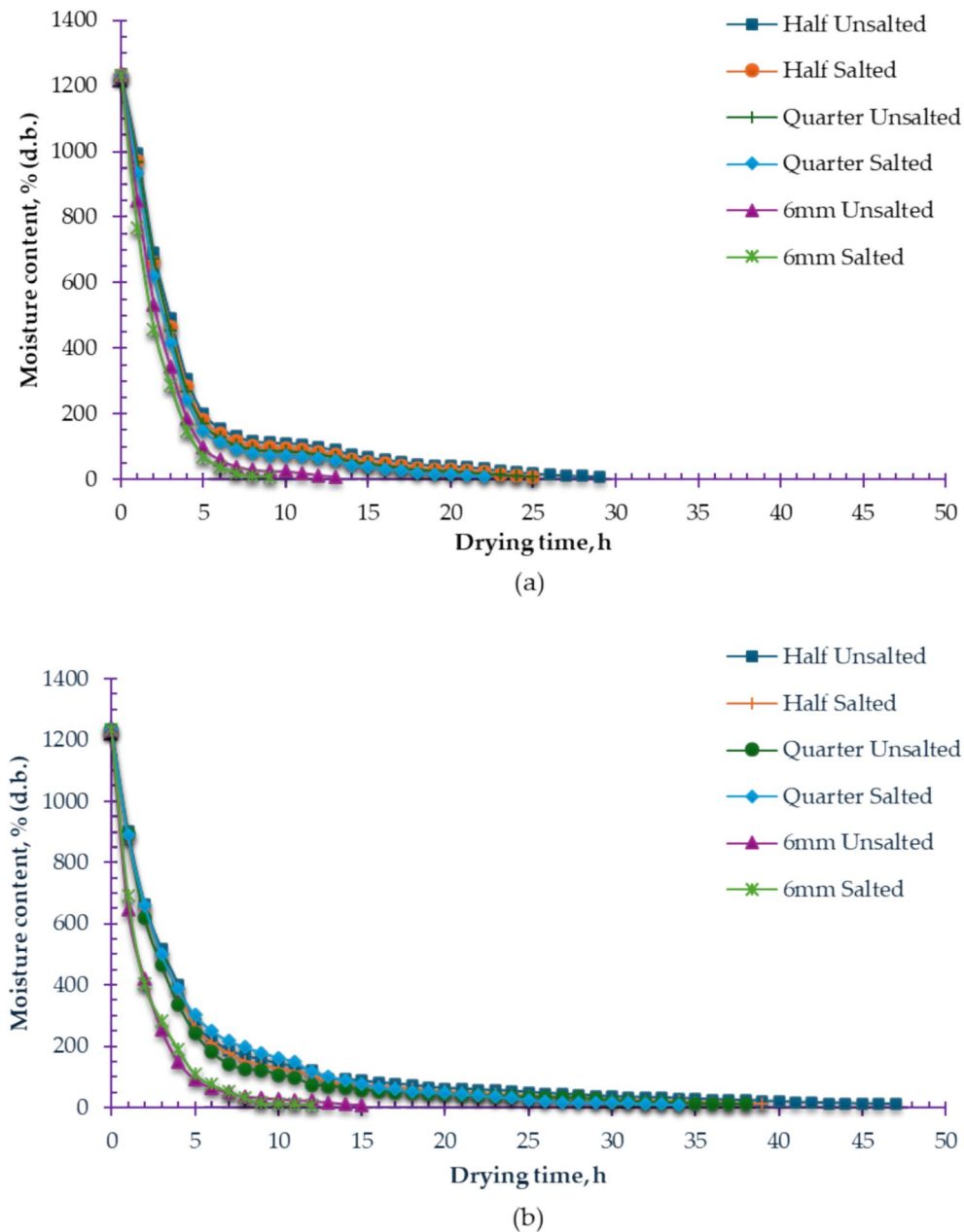


Fig. 8. MC of different tomato samples dried using both drying methods (DDS (a) and OSD (b)).

In contrast, the DDS significantly reduced this duration to between 9 and 29 h. This demonstrates a reduction in drying time of roughly 25% to 39.6% when using the DDS under the same sample shape and salting conditions. Moreover, salted samples consistently dried faster than their unsalted counterparts. For instance, the shortest drying time observed using the DDS was 9 h for salted slices (6 mm), while the longest was 29 h for unsalted halves. Salting reduced the drying duration by approximately 0.25%, 12%, and 13.8% for slices, quarters, and halves, respectively. Zambare and Kulkarni stated that pretreatment of tomato sample treated with 10% salt solution for 10 min soaking time exhibited the best sensory attributes⁹⁰. Also, Yanniotis et al.⁹¹ reported that salting tomatoes before drying reduces drying time by about 20% compared to unsalted tomatoes under the same conditions⁹². The physical form of the tomato also had a significant impact on the drying rate. Samples sliced to 6 mm thickness required only 9 to 13 h to dry using the DDS, while quartered samples took about 22 to 25 h, and halved samples needed 25 to 29 h. These results highlight the importance of both salting and sample geometry in optimizing the drying process efficiency using solar drying technologies. Many previous studies indicated that, solar drying significantly reduces drying time compared to traditional sun drying, with advanced systems (e.g., solar concentrators, forced convection, or sun-tracking collectors) achieving up to 21–25% faster drying and higher internal temperatures, which accelerates moisture removal^{20,93,94}. Also, slice thickness and shape matter: Thinner slices (e.g., 4 mm) dry much faster, with up to 50% reduction in drying time compared to thicker slices^{20,95}.

Table 5 presents the values of the drying coefficient (k_D) and the R^2 for tomatoes dried using two distinct drying systems—SDDSD and OSD. The experiments were conducted across three different physical configurations of the tomatoes: halves, quarters, and 6 mm thick slices, and under two salting conditions: salted and unsalted. The results clearly show that the k_D increases with higher drying air temperatures in the DDS, indicating enhanced moisture removal rates under elevated thermal conditions. According to the DDS, the highest k_D was about 0.5843, and it was observed for salted tomato slices, indicating rapid moisture diffusion due to both increased surface area and the hygroscopic effect of salting. In contrast, the lowest k_D was about 0.1425, and it was recorded with unsalted tomato halves, which have a lower surface-to-volume ratio and slower moisture migration. A similar trend was observed for the OSD, where the highest k_D was about 0.4186, and it was also found in salted slices, while the lowest value was about 0.0811, and it was seen in unsalted halves. These results confirm that both geometry and salting play a crucial role in drying kinetics, with thinner, salted samples achieving significantly faster drying rates than larger, unsalted ones. In terms of model fit, the R^2 values were generally high across all configurations, indicating a strong correlation between experimental and predicted data. The maximum R^2 value—0.9935—was obtained for salted tomato slices dried using the DDS, reflecting excellent model accuracy and consistency in this configuration. These findings are consistent with those reported in previous studies^{36,96–98}, further validating the influence of product geometry, salting, and drying system on the drying behavior of agricultural products like tomatoes.

Figure 9 illustrates the variation in drying method, physical shape, and salting condition concerning the MR of tomato slices. The MR is a dimensionless quantity used to express the relative amount of moisture remaining in a material during the drying process, compared to its initial MC. It helps standardize drying data, making it easier to compare different drying conditions or systems. As solar radiation increased throughout the day—from a low of 88 W/m² to a peak of 826 W/m²—the MR of the tomato samples gradually decreased. This decline was more pronounced in the DDS compared to the OSD. The accelerated moisture loss in the DDS is attributed to both the high initial MC of the tomato samples (approximately 92.5%) and the system's superior ability to absorb and retain thermal energy. The elevated temperatures within the DDS enhanced the evaporation process, leading to a faster reduction in MC. However, as solar radiation declined during the later hours of the day, the rate of moisture removal slowed, and the overall drying time increased. This inverse relationship between solar irradiance and drying duration underscores the dependency of the drying process on consistent thermal input. The drying of high-moisture agricultural products such as tomatoes typically occurs in two distinct phases. In the initial phase, also known as the constant rate period, moisture removal is rapid due to the abundance of surface water. During this stage, a portion of the absorbed thermal energy facilitates the evaporation of surface moisture, while the remainder penetrates the product to raise its internal temperature. This internal heating enhances capillary action, allowing water molecules to migrate from the interior toward the surface, where they are removed via external mass transfer mechanisms. As drying progresses into the falling rate period, surface moisture diminishes, and moisture migration from the interior becomes the rate-limiting step. In this phase, internal diffusion dominates the drying kinetics. Furthermore, reducing the sample thickness and applying salting significantly accelerate the drying process. Thinner samples provide a larger surface-area-to-volume ratio, which enhances heat and mass transfer, while salting alters the osmotic gradient and draws out internal moisture more efficiently. Together, these factors facilitate faster attainment of the equilibrium MC and reduce the total drying time.

DR refers to the speed at which moisture is removed from a material—typically expressed as the amount of water evaporated per unit time and per unit mass or area of the material. It's critical for designing and optimizing drying systems (e.g., SDs, industrial dryers). And It helps in understanding drying kinetics, which affect product quality, efficiency, and cost. A higher DR means the product dries faster, which can save energy and time. The relationship between DR and MC for various tomato samples—considering both drying systems, different physical shapes, and salting status—is illustrated in Fig. 10. The plotted data clearly indicates that the DR was at its peak during the initial stages of drying and then gradually declined. This trend suggests that the majority of moisture loss occurred during the falling rate period, aligning with findings reported in previous studies^{14,66,99–112}. For the DDS, the highest DR was recorded for salted tomato halves at approximately 360 g_{water}/g_{dry matter} h, followed by salted tomato quarters at around 350 g_{water}/g_{dry matter} h. Conversely, the lowest DR was observed for unsalted tomato slices, which reached only 210 g_{water}/g_{dry matter} h. While for the OSD, the highest DR was recorded for salted tomato halves at approximately 162 g_{water}/g_{dry matter} h, followed by salted tomato quarters and slices at around 130 g_{water}/g_{dry matter} h. Conversely, the lowest DR was observed for unsalted tomato slices, which reached only 80 g_{water}/g_{dry matter} h. Additionally, the results highlight that the physical shape of the tomato samples had the most pronounced effect on the DR across both systems. In contrast, the difference in DR between salted and unsalted samples was relatively minor, indicating that sample geometry plays a more dominant role than salting in influencing the drying kinetics.

Items	Open sun drying (OSD)						Developed direct SD (DDS)					
	Half		Quarter		6 mm		Half		Quarter		6 mm	
	Unsalted	Salted	Unsalted	Salted	Unsalted	Salted	Unsalted	Salted	Unsalted	Salted	Unsalted	Salted
k_D	0.0811	0.1006	0.1032	0.1293	0.2970	0.4186	0.1425	0.1625	0.1657	0.1965	0.3762	0.5843
R^2	0.9336	0.9385	0.9156	0.9789	0.9419	0.9862	0.9466	0.9385	0.9363	0.9417	0.9601	0.9935

Table 5. Drying coefficient (k_D) and coefficient determination (R^2) at different levels of different tomato samples dried using both drying methods (DDS (a) and OSD (b)).

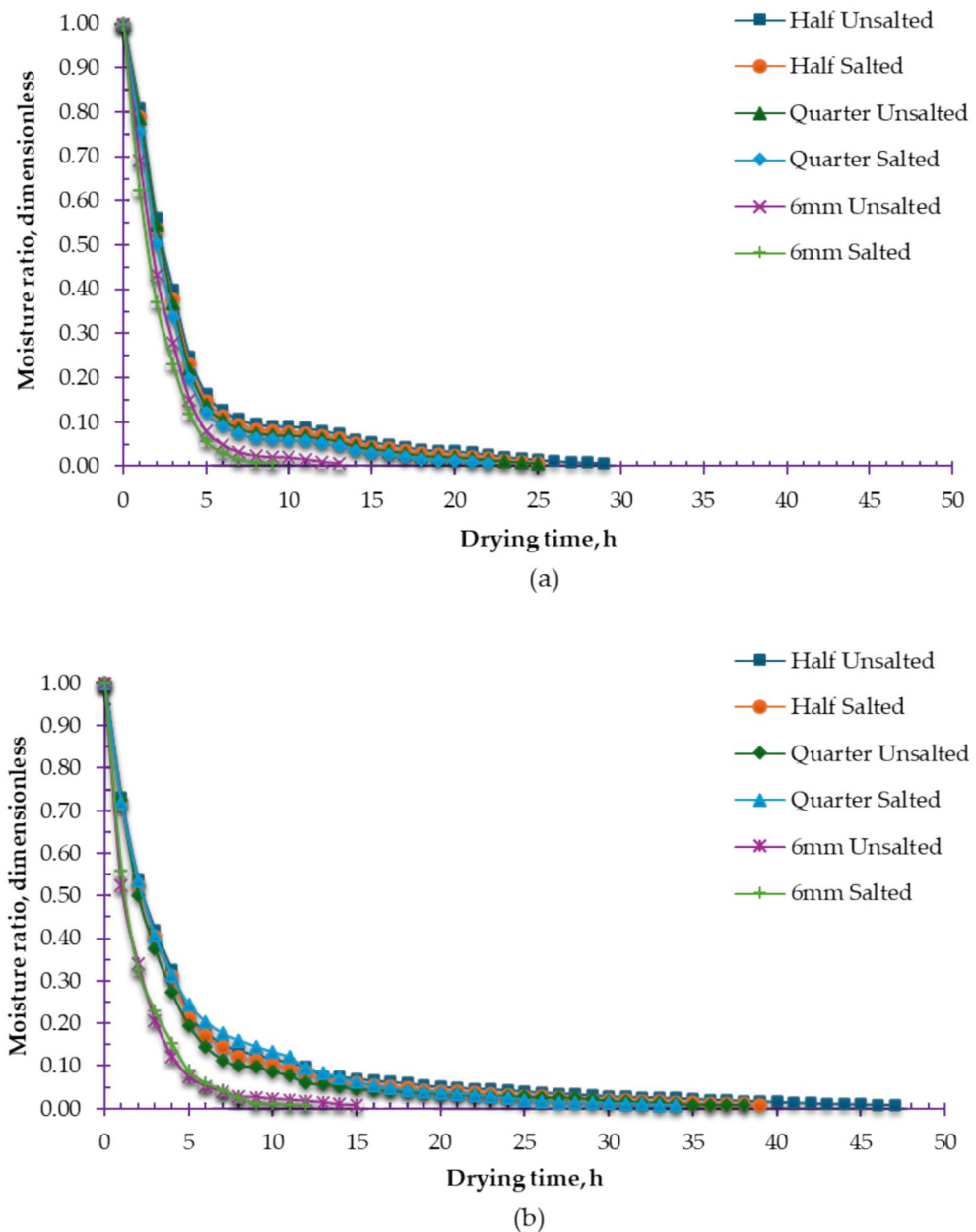


Fig. 9. MR of different tomato samples dried using both drying methods (DDSD (a) and OSD (b)).

The experimental MR data were analyzed to generate plots of the natural logarithm of the moisture ratio [$\ln(\text{MR})$] versus drying time (t), as illustrated in Fig. 11. These plots revealed a clear linear relationship between drying time and the natural logarithm of the MR. In drying process modeling, a primary experimental indicator is the reduction in sample mass, commonly expressed as the ratio of the MC at a given time (t) to the initial MC¹¹³. Figure 12 presents the D_{eff} values for tomato samples of varying physical shapes and salting conditions. The results clearly indicate that drying time is predominantly governed by internal mass transfer resistance, which is significantly affected by the presence of a falling-rate drying period. As a result, the D_{eff} under various experimental conditions was determined using Fick's second law of diffusion. As illustrated in Fig. 12, the salted tomato samples exhibited the highest D_{eff} values across both drying systems and for all physical shapes of tomato. The maximum D_{eff} recorded was approximately $5.92 \times 10^{-9} \text{ m}^2/\text{s}$ for salted tomato slices dried using the DDSD system, followed closely by salted tomato halves, with a D_{eff} of about $5.78 \times 10^{-9} \text{ m}^2/\text{s}$. Where salting likely disrupts the tomato tissue structure, making it easier for water to move out during drying. This effect is observed across different drying systems and physical shapes of tomato samples, indicating that the benefit of salting is robust and not limited to a specific drying method or sample geometry^{114–116}. The physical shape of the tomato samples significantly influenced the D_{eff} values, with sliced tomatoes consistently showing higher D_{eff} than halved samples in both drying methods. Overall, the D_{eff} values for tomato samples dried using the DSD system ranged from 1.82×10^{-9} to $5.92 \times 10^{-9} \text{ m}^2/\text{s}$, while those dried using the OSD system ranged from

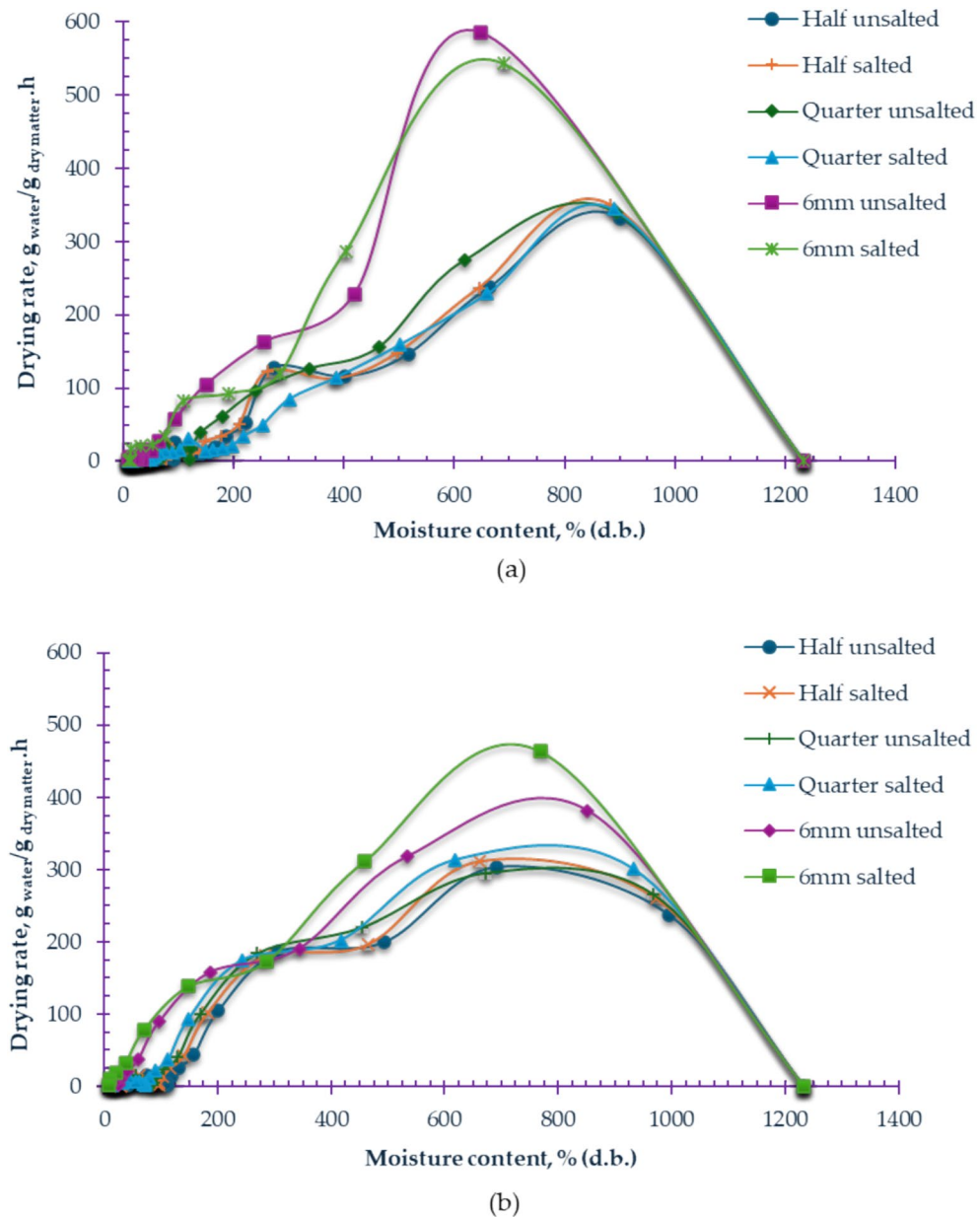
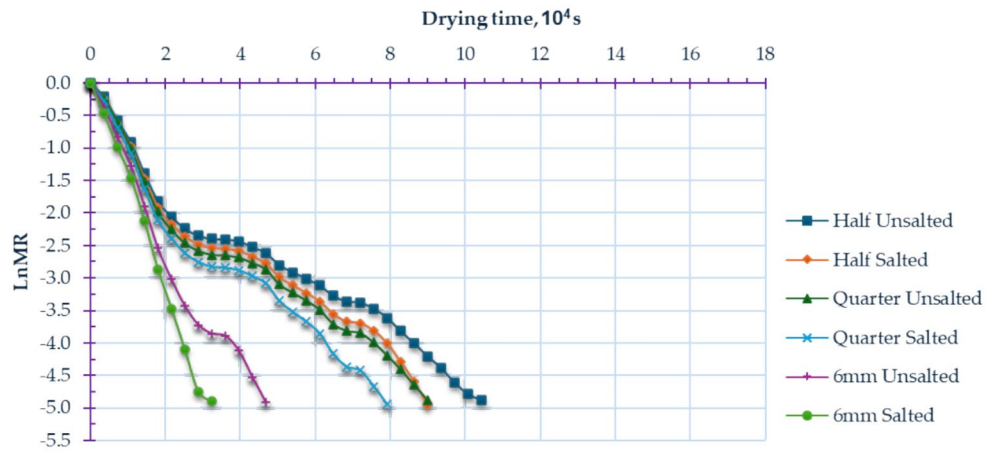


Fig. 10. Relation between MC and DR for different tomato samples dried using both drying methods (DDSD (a) and OSD (b)).

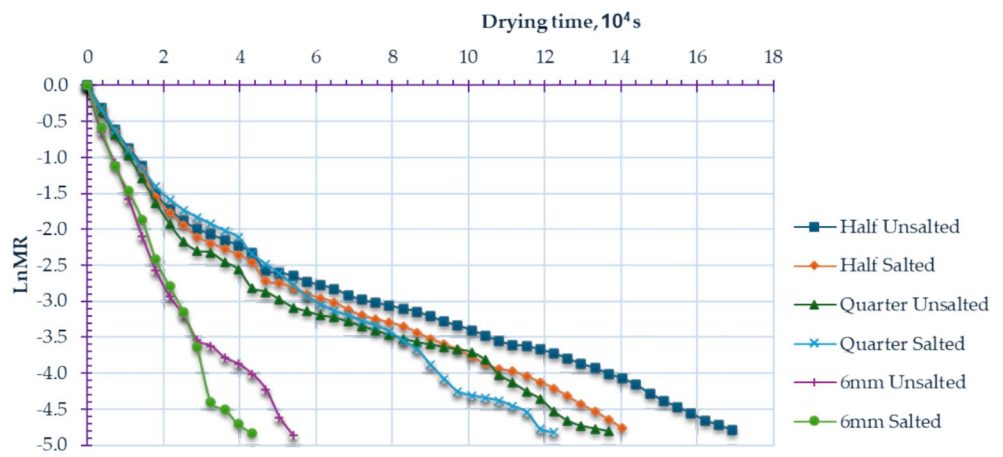
1.13×10^{-9} to 4.24×10^{-9} m²/s. These findings highlight the critical impact of both salting and sample geometry on internal moisture transfer during the drying process. The obtained data come in agreement with previous studies. For example, in oven drying of tomato halves, salted samples consistently showed higher D_{eff} values at all tested temperatures (45, 55, and 65 °C) than non-salted samples. At 65 °C, the D_{eff} for salted tomato halves was 4.0×10^{-10} m²/s, compared to 3.2×10^{-10} m²/s for non-salted ones, even when accounting for shrinkage effects. This means that salt treatment enhances the rate at which water diffuses out of the tomato, regardless of the physical shape (e.g., halves, slices) or the drying system used¹¹⁵. Table 6 shows a comparison between the obtained D_{eff} with previous drying studies of tomato.

Mathematical modeling of thin layer drying

Tables 7 and 8 summarize the constants of the applied mathematical models and the associated goodness-of-fit indicators for tomato samples dried using both the OSD and DDSD systems, taking into account variations in physical shape and salting status. MC data obtained from the drying experiments were analyzed using standard methodologies. The MC values were converted into MR expressions, and a total of twenty different drying models were applied for curve-fitting purposes. Statistical analysis revealed that all tested models demonstrated strong correlations with the experimental data, as indicated by high R^2 , as shown in Tables 7 and 8. In this study, R^2 , χ^2 , and RMSE were used as performance metrics to assess the accuracy of model fitting. Based on previous



(a)



(b)

Fig. 11. LnMR vs drying time for different tomato samples dried using both drying methods (DDSD (a) and OSD (b)).

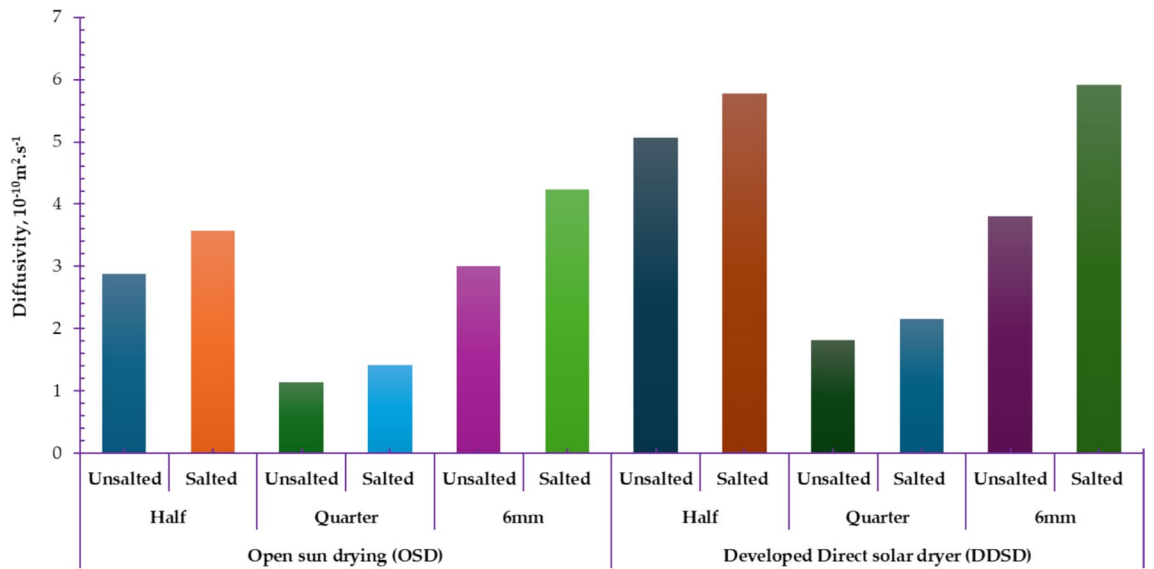


Fig. 12. D_{eff} for different tomato samples dried using both drying methods.

Dryer type	Solar collector type	Temperature (°C)	Air speed (m/s)	D_{eff} (m ² /s)	Key notes	Ref
Indirect SD	Not specified	Not specified	Not specified	3.60×10^{-9}	Mass transfer and heat transfer coefficients reported; collector efficiency 59.05%	117
Tracking indirect SD (PV-powered)	Fixed & tracking collector motion	Not specified	1, 1.5, 2	$7.15\text{--}9.30 \times 10^{-10}$	Higher D_{eff} with tracking collector; slice thickness also varied	19
Twin layer solar tunnel dryer	Not specified	Not specified	Not specified	Higher than OSD	Page model best fit; significant reduction in drying time	118
Hot air SD (swivel collector)	Swivel collector	Not specified	0.5, 1, 2	$1.58\text{--}6.98 \times 10^{-9}$	D_{eff} increased with air speed and slice thickness	119
Hybrid SD	Not specified	50–70	0.1–2	$3.87\text{--}9.63 \times 10^{-9}$	D_{eff} increased with air speed and temperature	120
Indirect forced convection SD	Flat plate collector	33 avg	Not specified	2.97×10^{-7}	Polynomial model best fit; collector efficiency 45–66%	121
Direct SD with heat recovery & PCM	Not specified	Not specified	Not specified	Not specified	50% reduction in drying time with PCM; effective D_{eff} modeled	122
DDSD	Direct solar collector	24.6–49.2	0.13 m ³ /s	$1.82\text{--}5.92 \times 10^{-9}$	Salted tomato slices had highest D_{eff}	Current study

Table 6. Comparison between the obtained D_{eff} with previous drying studies of tomato.

research^{123–125}, the most appropriate drying model is typically identified by the highest R^2 value and the lowest χ^2 and RMSE values, which together indicate a close agreement between predicted and actual data. Several models provided a good fit across the different tomato samples. According to the results in Table 7, for the OSD system, the Combined Two-term and Page model was the most accurate, achieving an R^2 of 0.999349, a χ^2 of 8.29×10^{-5} , and an RMSE of 0.007142. Meanwhile, for the DDSD system, the best-performing model was the Logistics model, as shown in Table 8, with an R^2 of 0.999524, a χ^2 of 6.74×10^{-5} , and an RMSE of 0.006868. Figures 13 and 14 compare the experimental MR (MR_{exp}) with the predicted values (MR_{pre}) over drying time for the best-fitting model (Logistics) applied to both drying systems.

Economic analysis

The performance evaluation of the DDSD provides a comprehensive quantitative analysis of the economic viability of this crop drying technology. This assessment serves as a valuable tool for policymakers, agricultural investors, and food industry stakeholders to make informed decisions regarding the adoption and implementation of sustainable drying solutions. The analysis was based on Eqs. 14 through 21, incorporating a lifetime reduction approach that accounts for the basic recovery process of the system's cost over time. Key variables influencing the system's performance and cost-efficiency were examined, as outlined in Tables 9 and 10. These variables were analyzed within the broader context of Egypt's current economic conditions and anticipated expenses associated with the various components of the DDSD.

As shown in Table 9, the initial capital investment required for the DDSD, when integrated with a PV power supply system, is approximately 520 USD. This figure is notably lower compared to the capital costs of conventional or alternative drying technologies. Furthermore, the DDSD system is designed with a projected operational lifespan of 20 years, underscoring its long-term cost-effectiveness and durability. The annualized capital cost and investment cost were calculated to be 106.79 USD and 101.45 USD, respectively, indicating favorable economic performance and justifying its feasibility as a sustainable drying solution in regions with similar economic and climatic conditions.

Table 10 highlights the most favorable payback periods across various combinations of tomato physical shapes and salting conditions, with the bolded figures in colored cells indicating the lowest values. The results clearly demonstrate that salting the tomato samples significantly improved the economic efficiency of the drying process. Specifically, the shortest payback periods were recorded for salted samples in all tested shapes—2.061 years for salted halves, 2.013 years for salted quarters, and 1.821 years for salted slices. This reduction in payback period can be attributed to the positive impact of salting on the drying kinetics. Salting enhances mass transfer during drying, thereby shortening the overall drying time. As a result, more batches can be processed within the year, which increases the total annual production of dried tomatoes and accelerates the return on investment. Moreover, the physical shape of the tomato samples was found to play a significant role in economic performance. Among all shapes tested, tomato slices exhibited the most favorable results, yielding the lowest payback period of 1.821 years when salted. This is primarily due to their thin structure, which requires the shortest drying time, only 9 h—allowing for higher throughput and greater annual output compared to quarters and halves. In essence, the combination of salting and slicing not only optimizes the drying efficiency but also enhances the economic viability of the process, making it the most effective strategy for rapid cost recovery.

Environmental analysis

Conducting an environmental impact assessment of the DDSD integrated with a PV system is crucial to evaluating its sustainability and long-term benefits. Table 11 presents the embodied energy associated with the various materials used in the construction of the DDSD. The total embodied energy was calculated to be approximately 1962.685 kWh, while the corresponding lifetime CO₂ emissions amounted to 133.46 metric tons (Table 11), reflecting the energy and environmental costs embedded in the manufacturing and installation of the system. The analysis further reveals that the annual energy output, defined as the energy used for the evaporation of water from tomato samples, was significantly higher for salted tomatoes compared to their unsalted counterparts. Among all sample types, tomato slices exhibited the greatest drying efficiency and annual energy output, primarily due to their reduced thickness and shorter drying time. As a result, the DDSD system,

Model	Physical shape	Salting status	Drying and models constants								Statistical indicators				
			k	a	b	c	d	g	h	L	n	R ²	χ ²	RMSE	
Newton (Lewis)	Half	Unsalted	0.300397									0.978383	0.001245	0.034694	
		Salt	0.321271									0.983102	0.001060	0.031919	
	Quarter	Unsalted	0.329868									0.984251	0.000996	0.030946	
		Salt	0.359513									0.988961	0.000739	0.026592	
	6 mm	Unsalted	0.436957									0.995885	0.000383	0.018866	
		Salt	0.504533									0.998123	0.000207	0.013641	
Page	Half	Unsalted	0.315161								0.962731	0.978532	0.001280	0.034557	
		Salt	0.318555								1.006882	0.983110	0.001103	0.031913	
	Quarter	Unsalted	0.301334								1.075105	0.984857	0.000999	0.030365	
		Salt	0.328052								1.079892	0.989672	0.000725	0.025734	
	6 mm	Unsalted	0.372078								1.155021	0.999027	0.000098	0.009175	
		Salt	0.462196								1.094139	0.999480	0.000064	0.007182	
Simplified ficks diffusion	Half	Unsalted		1.020084		0.676355					1.484889	0.978706	0.001317	0.034431	
		Salt		1.021443		0.701655					1.461866	0.983488	0.001125	0.031548	
	Quarter	Unsalted		1.028047		0.716640					1.453727	0.984907	0.001037	0.030290	
		Salt		1.023578		0.771459					1.448273	0.989445	0.000777	0.025999	
	6 mm	Unsalted		1.022442		0.798546					1.338496	0.996396	0.000397	0.017657	
		Salt		1.010699		0.819387					1.268389	0.998258	0.000247	0.013142	
Approximation or diffusion or diffusion approach	Half	Unsalted	0.300397	1.000000	1.000000							0.978383	0.001337	0.034694	
		Salt	0.321271	1.000000	1.000000							0.983102	0.001152	0.031919	
	Quarter	Unsalted	0.329868	1.000000	1.000000							0.984251	0.001083	0.030946	
		Salt	0.359513	1.000000	1.000000							0.988961	0.000813	0.026592	
	6 mm	Unsalted	0.436957	1.000000	1.000000							0.995885	0.000453	0.018866	
		Salt	0.504533	1.000000	1.000000							0.998123	0.000266	0.013641	
Combined two-term and page	Half	Unsalted	0.338304	0.515738	0.515738					0.338304	0.932100	0.979176	0.001389	0.034017	
		Salt	0.337417	0.512311	0.512311					0.337417	0.980232	0.983522	0.001229	0.031509	
	Quarter	Unsalted	0.317579	0.510285	0.510285					0.317579	1.048805	0.985137	0.001120	0.030072	
		Salt	0.339752	0.507176	0.507176					0.339752	1.061879	0.989817	0.000834	0.025548	
	6 mm	Unsalted	0.372548	0.500271	0.500271					0.372548	1.154318	0.999027	0.000131	0.009174	
		Salt	0.460695	0.499172	0.499172					0.460695	1.095951	0.999482	0.000103	0.007163	
Modified henderson and pabis	Half	Unsalted	0.306751	0.340028	0.340028	0.340028		0.306751	0.306751			0.978706	0.001482	0.034431	
		Salt	0.328327	0.340481	0.340481	0.340481		0.328327	0.328327			0.983488	0.001294	0.031548	
	Quarter	Unsalted	0.339106	0.342682	0.342682	0.342682		0.339106	0.339106			0.984907	0.001193	0.030290	
		Salt	0.367798	0.341192	0.341192	0.341192		0.367798	0.367798			0.989445	0.000915	0.025999	
	6 mm	Unsalted	0.445725	0.340814	0.340814	0.340814		0.445725	0.445725			0.996396	0.000546	0.017657	
		Salt	0.509312	0.336899	0.336899	0.336899		0.509312	0.509312			0.998258	0.000432	0.013142	
Modified midilli II	Half	Unsalted	0.271210	0.974145	0.038657						1.194755	0.991180	0.000563	0.022096	
		Salt	0.281540	0.970791	0.037633						1.217891	0.994120	0.000417	0.018788	
	Quarter	Unsalted	0.268992	0.970774	0.034554						1.269585	0.994985	0.000359	0.017432	
		Salt	0.305036	0.973568	0.030084						1.231682	0.996685	0.000256	0.014555	
	6 mm	Unsalted	0.371427	0.984729	0.009787						1.173915	0.999444	0.000067	0.006934	
		Salt	0.460693	0.998339	0.000000						1.095947	0.999482	0.000086	0.007163	
Modified page III	Half	Unsalted	1.020084							1.484889		0.676355	0.978706	0.001317	0.034431
		Salt	1.021443							1.461866		0.701655	0.983488	0.001125	0.031548
	Quarter	Unsalted	1.028047							1.453727		0.716640	0.984907	0.001037	0.030290
		Salt	1.023578							1.448273		0.771459	0.989445	0.000777	0.025999
	6 mm	Unsalted	1.022442							1.338496		0.798546	0.996396	0.000397	0.017657
		Salt	1.010699							1.268389		0.819387	0.998258	0.000247	0.013142
Modified two term III	Half	Unsalted	0.300397	1.000001								0.978383	0.001290	0.034694	
		Salt	0.321271	1.000001								0.983102	0.001104	0.031919	
	Quarter	Unsalted	0.329868	1.000001								0.984251	0.001037	0.030946	
		Salt	0.359513	1.000001								0.988961	0.000774	0.026592	
	6 mm	Unsalted	0.436957	1.000001								0.995885	0.000415	0.018866	
		Salt	0.504533	1.000001								0.998123	0.000233	0.013641	

Continued

Model	Physical shape	Salting status	Drying and models constants								Statistical indicators			
			k	a	b	c	d	g	h	L	n	R ²	χ ²	RMSE
Logistics	Half	Unsalted	0.309761	597.7731	616.4038							0.978622	0.001322	0.034496
		Salt	0.329478	341.4494	350.3175							0.983479	0.001126	0.031558
	Quarter	Unsalted	0.362023	7.907679	9.120310							0.984988	0.001032	0.030218
		Salt	0.410456	4.409927	5.497925							0.989689	0.000760	0.025707
	6 mm	Unsalted	0.582847	1.371266	2.373732							0.999068	0.000103	0.008978
		Salt	0.605352	2.407269	3.401762							0.999524	0.000067	0.006868
Logarithmic (asymptotic)	Half	Unsalted	0.343830	1.007626		0.031099						0.988829	0.000687	0.024867
		Salt	0.363347	1.008208		0.028665						0.991031	0.000609	0.023204
	Quarter	Unsalted	0.368722	1.015766		0.024511						0.990506	0.000650	0.023985
		Salt	0.394004	1.012462		0.020494						0.993028	0.000512	0.021109
	6 mm	Unsalted	0.445723	1.022442		0.000000						0.996396	0.000397	0.017657
		Salt	0.509317	1.010697		0.000000						0.998258	0.000247	0.013142
Parabolic model	Half	Unsalted	0.677268		-0.073467	0.001874						0.784651	0.013245	0.109182
		Salt	0.828761		-0.107673	0.003236						0.785931	0.014579	0.113566
	Quarter	Unsalted	0.828540		-0.108946	0.003291						0.780886	0.015065	0.115441
		Salt	0.804550		-0.118720	0.004038						0.819808	0.013263	0.107391
	6 mm	Unsalted	0.870090		-0.202183	0.011027						0.943375	0.006234	0.069986
		Salt	0.921012		-0.279859	0.020535						0.976898	0.003271	0.047850

Table 7. Mathematical models drying and models constants and statistical indicators for DDSD of tomatoes.

when used for drying salted tomato slices, achieved the highest annual yield of dried product, leading to several environmental and economic advantages. This configuration maximized the net carbon dioxide mitigation over the system's lifetime, reaching 105.68 tons, and reduced the EPBT—the time required for the system to generate an amount of energy equal to what was used in its production—to just 1.10 years. Moreover, the environmental benefits translated into financial gains through carbon credits. The DDSD system, operating under optimal conditions (drying salted tomato slices), was estimated to earn approximately 1321.04 USD in carbon credits over its lifetime, highlighting its potential not only as a sustainable drying technology but also as a cost-effective investment in terms of environmental impact reduction and carbon trading opportunities. Table 12 shows the comparison between EPBT of our DDSD with other similar models.

Conclusion

During the current investigation, a comprehensive comparative study was carried out to evaluate the drying performance of tomatoes using two distinct methods: the DDSD and traditional OSD. The experiments were conducted on tomato samples prepared in three different physical forms—halves, quarters, and slices of 6 mm thickness. Each form was further subjected to two pretreatment conditions: salted and unsalted. All drying trials were initiated with an average initial MC of approximately 92.5% on a dry basis, ensuring consistency across the dataset. Key findings from the study include the following:

- The final EMC values of the dried tomatoes varied between 8.7% and 9.5% (d.b.) for samples dried using the OSD method, whereas tomatoes dried using the DDSD achieved slightly lower EMCs ranging from 7.9% to 8.6% (d.b.), indicating more effective moisture removal in the DDSD system.
- The DDSD system significantly enhanced the drying kinetics. The highest DR, recorded for salted tomato halves dried using DDSD, reached 360 g of water per gram of dry matter per hour. Furthermore, the use of DDSD reduced the total drying duration by approximately 39.6% compared to the OSD method, demonstrating its superior performance in achieving rapid dehydration under controlled conditions.
- For salted tomato slices, the D_{eff} during drying using the DDSD was calculated to be around $5.92 \times 10^{-9} \text{ m}^2/\text{s}$. This value underscores the favorable internal moisture transport characteristics of the DDSD setup, which enhances drying uniformity and efficiency.
- Among the 12 mathematical models tested for describing the drying behavior, the Logistic model provided the best fit for the experimental data obtained from tomato samples dried in the DDSD. This suggests its suitability for predicting drying kinetics under similar operational conditions.
- The DDSD system integrated with a PV power source was found to be economically feasible. With a relatively low capital investment of \$520, the system yielded a payback period as short as 1.82 years, particularly for salted tomato slices. This rapid return on investment is attributed to increased drying capacity and substantial time savings.
- From a sustainability perspective, the DDSD presents notable environmental advantages. Over a projected operational life of 20 years, it is estimated to prevent the emission of approximately 105.68 metric tons of CO₂, relative to equivalent grid-powered drying processes. The EPBT was calculated at only 1.10 years, indicating swift energy recovery. Additionally, the system offers potential economic gains through environmental credits, estimated at \$1321.04 from carbon offset programs.

Model	Physical shape	Salting status	Drying and models constants									Statistical indicators				
			k	a	b	c	d	g	h	L	n	R ²	χ ²	RMSE		
Newton (Lewis)	Half	Unsalted	0.266003										0.967927	0.001203	0.034322	
		Salt	0.281726										0.977054	0.000977	0.030858	
	Quarter	Unsalted	0.309874										0.983191	0.000721	0.026497	
		Salt	0.258527										0.974031	0.001246	0.034794	
	6 mm	Unsalted	0.547352										0.994469	0.000394	0.019219	
		Salt	0.517835										0.995833	0.000354	0.018072	
Page	Half	Unsalted	0.408529								0.712898	0.986640	0.000506	0.022028		
		Salt	0.404681								0.750092	0.991067	0.000387	0.019183		
	Quarter	Unsalted	0.400979								0.807457	0.989711	0.000451	0.020679		
		Salt	0.391859								0.734706	0.995927	0.000200	0.013743		
	6 mm	Unsalted	0.633360								0.832757	0.998850	0.000088	0.008760		
		Salt	0.588007								0.863246	0.999349	0.000060	0.007142		
Simplified ficks diffusion	Half	Unsalted		0.946867		0.628978					1.587765		0.970132	0.001170	0.033118	
		Salt		0.952824		0.644414					1.554657		0.978883	0.000947	0.029603	
	Quarter	Unsalted		0.974816		0.676325					1.498140		0.983708	0.000737	0.026089	
		Salt		0.930075		0.618555					1.613997		0.978269	0.001108	0.031825	
	6 mm	Unsalted		0.978849		0.827424					1.242579		0.994930	0.000417	0.018403	
		Salt		0.980842		0.815046					1.266607		0.996237	0.000383	0.017175	
Approximation or diffusion or diffusion approach	Half	Unsalted	0.266003	1.000000	1.000000								0.967927	0.001257	0.034322	
		Salt	0.281726	1.000000	1.000000									0.977054	0.001029	0.030858
	Quarter	Unsalted	0.309874	1.000000	1.000000									0.983191	0.000761	0.026497
		Salt	0.258527	1.000000	1.000000									0.974031	0.001324	0.034794
	6 mm	Unsalted	0.547352	1.000000	1.000000									0.994469	0.000455	0.019219
		Salt	0.517835	1.000000	1.000000									0.995833	0.000425	0.018072
Combined two-term and page	Half	Unsalted	0.426523	0.512173	0.512173				0.426523		0.699046	0.987006	0.000527	0.021720		
		Salt	0.418457	0.509077	0.509077				0.418457		0.738624	0.991281	0.000410	0.018950		
	Quarter	Unsalted	0.415333	0.509196	0.509196				0.415333		0.794112	0.989931	0.000480	0.020453		
		Salt	0.402267	0.507014	0.507014				0.402267		0.726224	0.996057	0.000213	0.013521		
	6 mm	Unsalted	0.633240	0.499935	0.499935				0.633240		0.832845	0.998850	0.000112	0.008759		
		Salt	0.588064	0.500031	0.500031				0.588064		0.863202	0.999349	0.000083	0.007142		
Modified henderson and pabis	Half	Unsalted	0.249495	0.315622	0.315622	0.315622		0.249495	0.249495				0.970132	0.001254	0.033118	
		Salt	0.266622	0.317608	0.317608	0.317608		0.266622	0.266622					0.978883	0.001031	0.029603
	Quarter	Unsalted	0.301336	0.324939	0.324939	0.324939		0.301336	0.301336					0.983708	0.000804	0.026089
		Salt	0.237450	0.310025	0.310025	0.310025		0.237450	0.237450					0.978269	0.001222	0.031825
	6 mm	Unsalted	0.535897	0.326283	0.326283	0.326283		0.535897	0.535897					0.994930	0.000542	0.018403
		Salt	0.508042	0.326947	0.326947	0.326947		0.508042	0.508042					0.996237	0.000548	0.017175
Modified midilli II	Half	Unsalted	0.377462	0.985469	0.026651							0.828496	0.994193	0.000230	0.014507	
		Salt	0.380144	0.983453	0.024485							0.850711	0.996425	0.000163	0.012126	
	Quarter	Unsalted	0.375730	0.983292	0.024953							0.921023	0.996707	0.000152	0.011682	
		Salt	0.388678	0.996146	0.013826							0.771852	0.996925	0.000161	0.011940	
	6 mm	Unsalted	0.630001	0.988713	0.009906							0.871632	0.999277	0.000064	0.006944	
		Salt	0.578164	0.994219	0.000610							0.876204	0.999299	0.000079	0.007409	
Modified page III	Half	Unsalted	0.946867							1.587765			0.628978	0.970132	0.001170	0.033118
		Salt	0.952824							1.554657			0.644414	0.978883	0.000947	0.029603
	Quarter	Unsalted	0.974816							1.498140			0.676325	0.983708	0.000737	0.026089
		Salt	0.930075							1.613997			0.618555	0.978269	0.001108	0.031825
	6 mm	Unsalted	0.978849							1.242579			0.827424	0.994930	0.000417	0.018403
		Salt	0.980842							1.266607			0.815046	0.996237	0.000383	0.017175
Modified two term III	Half	Unsalted	0.266003	1.000002									0.967927	0.001229	0.034322	
		Salt	0.281726	1.000001										0.977054	0.001002	0.030858
	Quarter	Unsalted	0.309874	1.000001										0.983191	0.000740	0.026497
		Salt	0.258527	1.000002										0.974031	0.001284	0.034794
	6 mm	Unsalted	0.547352	1.000001										0.994469	0.000422	0.019219
		Salt	0.517835	1.000001										0.995833	0.000386	0.018072

Continued

Model	Physical shape	Salting status	Drying and models constants									Statistical indicators		
			k	a	b	c	d	g	h	L	n	R ²	χ ²	RMSE
Logistics	Half	Unsalted	0.242149	1606.792	1482.008							0.969615	0.001190	0.033404
		Salt	0.264745	6834.425	6471.764							0.978851	0.000949	0.029626
	Quarter	Unsalted	0.303184	3048.032	2991.569							0.983668	0.000739	0.026119
		Salt	0.253167	4855.432	4771.821							0.975859	0.001231	0.033546
	6 mm	Unsalted	0.535798	3457.128	3382.972							0.994927	0.000417	0.018409
		Salt	0.510431	2906.925	2865.553							0.996210	0.000386	0.017237
Logarithmic (asymptotic)	Half	Unsalted	0.291979	0.943458		0.033757						0.990716	0.000359	0.018342
		Salt	0.306562	0.946956		0.031436						0.993793	0.000276	0.015977
	Quarter	Unsalted	0.337864	0.966368		0.027889						0.996046	0.000178	0.012801
		Salt	0.276422	0.927801		0.031774						0.989401	0.000537	0.022166
	6 mm	Unsalted	0.573725	0.967626		0.018645						0.997677	0.000191	0.012447
		Salt	0.535290	0.972220		0.014513						0.997292	0.000276	0.014568
Parabolic model	Half	Unsalted		0.910344	-0.067959	0.001135						0.280345	0.029463	0.166198
		Salt		0.575942	-0.047191	0.000905						0.750863	0.011077	0.101224
	Quarter	Unsalted		0.888118	-0.082058	0.001692						0.442028	0.026001	0.154923
		Salt		0.875236	-0.084950	0.001892						0.682781	0.016381	0.122380
	6 mm	Unsalted		0.710369	-0.149767	0.007318						0.849587	0.012350	0.100172
		Salt		0.812978	-0.200773	0.011729						0.914816	0.008677	0.081699

Table 8. Mathematical models drying and models constants and statistical indicators for of open sun drying of tomatoes.

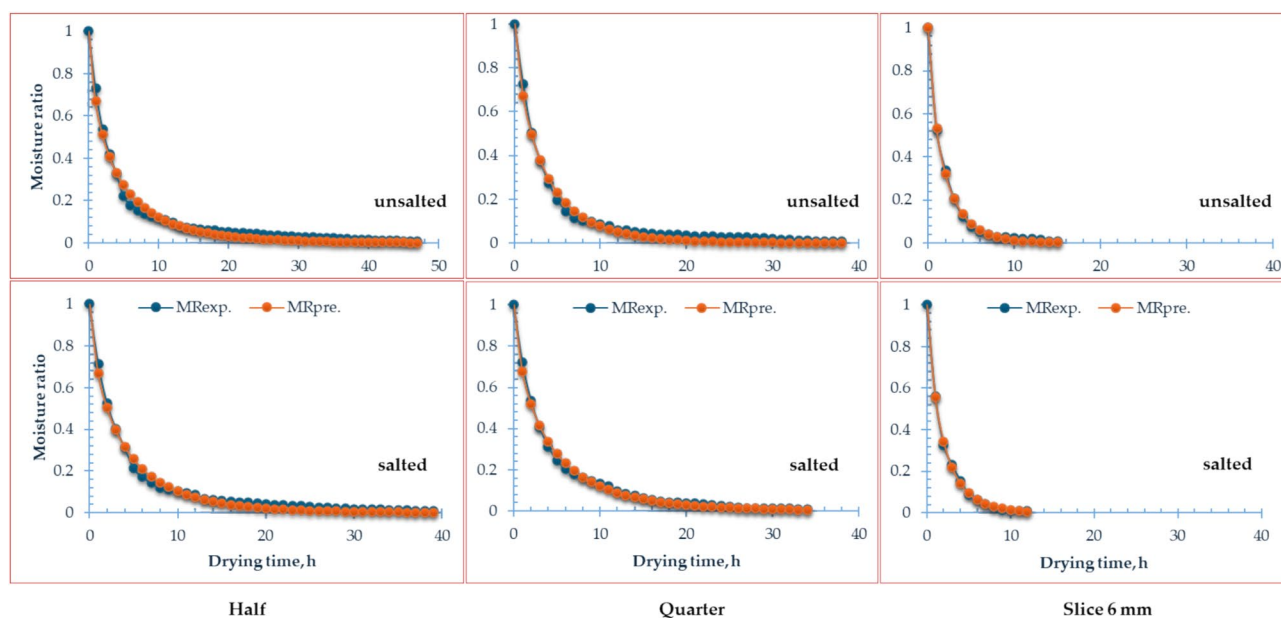


Fig. 13. Experimental (MR_{exp}) and predicted MR (MR_{pre}) versus drying time for the best mathematical model (Combined Two-term and Page) for open sun drying (OSD) of tomatoes.

In summary, the DDS system not only outperforms traditional OSD in terms of drying efficiency and product quality but also proves to be an economically sound and environmentally responsible technology for tomato dehydration, especially in solar-rich regions.

Limitations and future works

The study did not assess the effects of drying variables on the chemical composition and color of tomatoes, which are key quality indicators. Additionally, thermal analysis of the drying system was not conducted, limiting insights into heat distribution and energy efficiency. Future work should address these gaps.

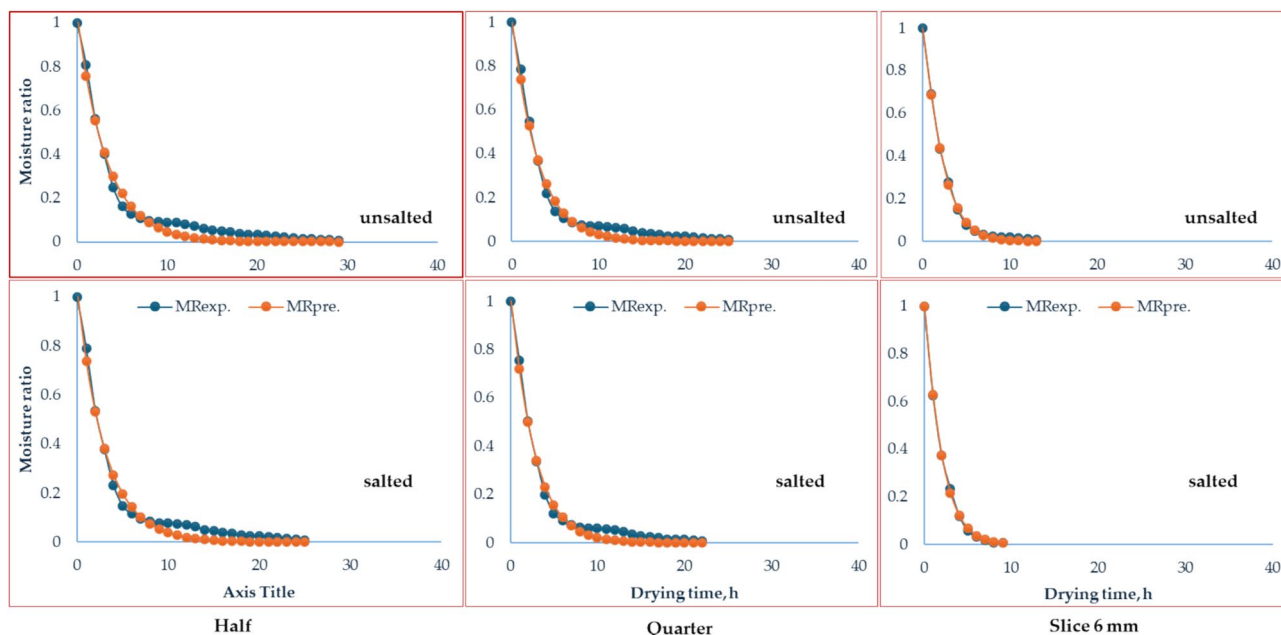


Fig. 14. Experimental (MR_{exp}) and predicted MR (MR_{pre}) versus drying time for the best mathematical model (Logistics) for tomato drying using the developed direct SD (DDSD).

Cost parameters	Value
Capital cost, USD	520
Lifespan, years	20
Annual capital cost, USD	106.79
Annual maintenance cost, USD	3.21
Annual salvage value, USD	8.54
Annualized investment cost, USD	101.45

Table 9. Various costs related to the DDSD integrated with PV system.

Economic analysis	Half		Quarter		6 mm	
	Unsalted	Salted	Unsalted	Salted	Unsalted	Salted
Dried quantity, kg/year (fresh weight)	2153.8	3111.1	2800	3181.8	3017.2	3500
Saving after 1 year	215.4	311.1	280	318.2	301.7	350
Payback period, year	3.054	2.061	2.305	2.013	2.129	1.821

Table 10. Economic parameters of the DDSD for drying tomato.

Environmental parameters	Half		Quarter		6 mm	
	Un-salted	Salted	Unsalted	Salted	Unsalted	Salted
Initial weight, g	7980	7500	19,320	19,200	24,000	23,100
Final weight, g	1260	1194	2406	2988	3858	3564
Initial MC, %	92.5	92.5	92.5	92.5	92.5	92.5
Final MC, %	8.4	8.3	8.6	8.1	8.6	7.9
EE, kW h	1962.69	1962.69	1962.69	1962.69	1962.69	1962.69
Total annual energy output, kW h	1184.47	1605.50	1485.92	1688.55	1591.49	1790.58
EPBT, year	1.66	1.22	1.32	1.16	1.23	1.10
Annual CO ₂ emissions, ton	133.46	133.46	133.46	133.46	133.46	133.46
Net CO ₂ mitigation per lifetime, ton	68.55	94.35	87.02	99.43	93.49	105.68
ECC, USD	856.91	1179.31	1087.75	1242.91	1168.58	1321.04

Table 11. Analysis of different environmental parameters.

References	Type of the SD	Product	EPBT, year
⁵⁰	Novel phase change material SD using paraffin wax, stearic acid, and acetamide for drying tomatoes	Tomato	2.51–2.98
¹²⁶	Three types of solar air heaters (finned plate, evacuated tube, and modified evacuated tube solar air heaters)	Eggplant & Grapes	1.27–8.41
¹²⁷	A mixed-mode SD equipped with a solar PV-powered dehumidifier	Agricultural products	2.70
¹²⁸	Grooved hybrid PVT-air collector dryer	Without load	2.98–3.51
¹²⁹	PV operated automatic SD	Dates	7.15
¹³⁰	PV operated large scale SD with phase change material energy storage	Without load	6.82
¹³¹	Indirectly forced convection desiccant integrated SD	Tomato	5.1396
¹³²	Indirect type domestic hybrid SD	Tomato	4.21
Current study	Forced air circulation, SD integrated with solar tracking flat plate solar collector	Tomato	2.40 years

Table 12. Comparison between EPBT of our DDSD with other similar models.

Data availability

All data are presented within the article.

Received: 31 May 2025; Accepted: 8 July 2025

Published online: 20 July 2025

References

- Mendoza-Buenrostro, E. et al. Effective use of microbial and plant-based alternatives in tomato pathogen control: A comprehensive review. *Plant Pathol.* **74**(5), 1171–1186 (2025).
- Verma, G. et al. Experimental investigation of mixed mode ultraviolet tent house SD under natural convection regime. *Sol. Energy* **251**, 51–67 (2023).
- Kumar, S., Ghritlahre, H. K., Agrawal, S. & Shekhar, S. An experimental investigation of active mixed-mode SD utilizing north wall reflector. *Energy Sources Part A Recovery Util. Environ. Eff.* **46**, 16813–16835 (2024).
- Dewangan, N. et al. An experimental investigation of mixed-mode tent house SD using ultraviolet sheet for drying potato slices. *Energy Sources Part A Recovery Util. Environ. Eff.* **45**, 11446–11466 (2023).
- Chabi, I. B. et al. Tomato pomace as a source of valuable functional ingredients for improving physicochemical and sensory properties and extending the shelf life of foods: A review. *Heliyon* **10**, e25261 (2024).
- Sattar, S. et al. Tomatoes unveiled: A comprehensive exploration from cultivation to culinary and nutritional significance. (Qeios, 2024).
- Yu, X., Yang, C. & Zhang, L. A novel tomato pulp with high cis-lycopene content and bioaccessibility through plant-derived sulfur-containing compounds in a simulated food system. *Food Res. Int.* **204**, 115915 (2025).
- Nikam, S. D. *Tomato Production and Marketing* (Ashok Yakkaldevi, 2025).
- Sharma, P., Divyanshu, K. K., Barwal, P. & Sharma, S. Economic viability of tomato cultivation in mid hills of Himachal Pradesh. *The Society of Economics and Development* **190** (2025).
- Govindasamy, R., Ceylan, R. F. & Özkan, B. Global tomato production: Price sensitivity and policy impact in Mexico, Türkiye, and the United States. *Horticulturae* **11**, 84 (2025).
- Dhotre, M., Nithin, K. N., Kolluru, R. & Desai, S. Recurring onion and tomato crises in India: A critical analysis and future perspectives. In *Emerging Trends in Food and Agribusiness Marketing* 123–160 (IGI Global, 2025).
- Du, M. et al. Molecular breeding of tomato: Advances and challenges. *J. Integr. Plant Biol.* **67**, 669–721 (2025).
- El-Dissoky, R., Sherif, A. & Mohamd, E. Agro-economic assessment of added fertilizers to tomato yield grown at Fayoum Governorate, Egypt. *J. Soil Sci. Agric. Eng. Mansoura Univ.* **9**, 771–780 (2018).
- Elwakeel, A. E. et al. Quality evaluation of dried tomato fruit and optimization of drying conditions using a modified SD integrated with an automatic solar collector tracker. *Sci. Rep.* **15**, 7659 (2025).
- Jana, G. A., Al-Kuwari, A. D., Al-Shamari, H. S. & Elazazi, E. Sustainable crop production in Qatar: A systemic review of tomato production (2025).

16. Gaviria-Lozano, A. C., Castro, A. M., Díaz, L. E., Quintanilla-Carvajal, M. X. & Moreno, F. L. Improving the drying efficiency, quality attributes, and lycopene bioaccessibility (in vitro) of tomato puree using refractance-window hybrid drying. *Innov. Food Sci. Emerg. Technol.* **102**, 4 (2025).
17. Eissa, A. S., Gameh, M. A., Mostafa, M. B. & Elwakeel, A. E. Some engineering factors affecting utilization of solar energy in drying tomato fruits. *Aswan Univ. J. Environ. Stud.* **5**, 52–68 (2024).
18. Elwakeel, A. E., Gameh, M. A., Eissa, A. S. & Mostafa, M. B. Recent advances in solar drying technology for tomato fruits: A comprehensive review. *Int. J. Appl. Energy Syst.* **6**, 37–44 (2024).
19. Elwakeel, A. et al. Drying kinetics and thermo-environmental analysis of a PV-operated tracking indirect SD for tomato slices. *PLoS ONE* **19**, e0306281 (2024).
20. Elwakeel, A. et al. Development and techno-economic analysis of a tracked indirect forced SD integrated photovoltaic system for drying tomatoes. *Sustainability*. <https://doi.org/10.3390/su16167008> (2024).
21. Kidane, H., Farkas, I. & Buzás, J. Characterizing agricultural product drying in solar systems using thin-layer drying models: Comprehensive review. *Discov. Food* **5**, 84 (2025).
22. Abdelhamid, M. A. et al. Design and evaluation of a solar powered smart irrigation system for sustainable urban agriculture. *Sci. Rep.* **15**, 11761 (2025).
23. Olanipekun, C. I. et al. Setting the stage for improved drying: A stepping stone to SD. (Intl Food Policy Res Inst, 2025).
24. Elmessery, W. M. et al. Deep regression analysis for enhanced thermal control in photovoltaic energy systems. *Sci. Rep.* **14**, 30600 (2024).
25. Khater, E. S. G. et al. Assessment of a LPG hybrid SD assisted with smart air circulation system for drying basil leaves. *Sci. Rep.* **14**, 23922 (2024).
26. Elwakeel, A. E., Tantawy, A. A., Alsebiey, M. M. & Elliby, A. K. The date fruit drying systems: A critical overview. *Al-Azhar J. Agric. Eng.* **2**, 26–36 (2022).
27. Mahmoud, W.A.E.-M. & Elwakeel, A. E. Study on some properties of tomato fruits for natural sun drying. *J. Soil Sci. Agric. Eng.* **12**, 763–767 (2021).
28. Fadeyibi, A. & Adewale, A. A. Enhancing osmo-dehydration process of sliced okra with non-ionizing radiation for quality improvement. *Discov. Food* **5**, 83 (2025).
29. Kumar, S. et al. Performance analysis of natural and forced convection mixed mode UV tent house SD for potato drying. *Energy Sources Part A Recover. Util. Environ. Eff.* **45**, 11482–11504 (2023).
30. Elwakeel, A. E. et al. Development, drying characteristics, and environmental analysis of a PV operated automatic SD for drying date. *Front Sustain. Food Syst.* **9**, 1531601 (2025).
31. Kumar, S., Ghritlahre, H. K., Agrawal, S. & Shekhar, S. Investigation of a novel mixed-mode SD using north wall reflector: An experimental study. *Sol. Energy* **282**, 112909 (2024).
32. Kumar, S. et al. Performance evaluation of cabinet SD using ultraviolet (UV) sheet. *Mater. Today Proc.* **56**, 2735–2741 (2022).
33. Ghanem, T. H. M. et al. Thin-layer modeling, drying parameters, and techno-enviro-economic analysis of a solar dried salted tilapia fish fillets. *Sci. Rep.* **15**, 5073 (2025).
34. Ambawat, S., Sharma, A. & Saini, R. K. Mathematical modeling of thin layer drying kinetics and moisture diffusivity study of pretreated *Moringa oleifera* leaves using fluidized bed dryer (2025).
35. Pandey, S., Kumar, A. & Sharma, A. Sustainable solar drying: Recent advances in materials, innovative designs, mathematical modeling, and energy storage solutions. *Energy* **308**, 132725 (2024).
36. Metwally, K. A. et al. The Mathematical modeling, diffusivity, energy, and enviro-economic analysis (MD3E) of an automatic SD for drying date fruits. *Sustainability* **16**, 3506 (2024).
37. Seerangurayar, T. et al. Experimental investigation and modeling of date drying under forced convection SDs. *Biomass Convers. Biorefin.* **14**, 21705–21718 (2024).
38. Ye, Y., Zhou, T., Liu, T. & Shi, W. Quality-based selection of the optimal hot air gradient drying method for anchovy and modeling of drying kinetics. *Aquac. Fish.* <https://doi.org/10.1016/j.aaf.2024.03.002> (2024).
39. Minaei, S. & Beheshti, B. Determining the effective diffusivity coefficient and activation energy in thin-layer drying of Haj Kazemi peach slices and modeling drying kinetics using ANFIS. *Int. J. Low Carbon Technol.* **19**, 192–206 (2024).
40. Hin, L. et al. Clean technologies development and performance assessment of sensor-mounted SD for micro-climatic modeling and optimization of dried fish quality in Cambodia. *Clean Technol.* **6**, 954–972 (2024).
41. Petru, C., Marius, B., Rat, R., Arsenoia, V. N. & Ros, G. R. Drying process modeling and quality assessments regarding an innovative seed dryer. *Agriculture* **13**, 328 (2023).
42. Daliran, A., Taki, M., Marzban, A., Rahnama, M. & Farhadi, R. Kinetic analysis, mathematical modeling and quality evaluation of mint drying in greenhouse SD. *Therm. Sci. Eng. Prog.* **46**, 102252 (2023).
43. Younis, O. S. et al. Drying characteristics, environmental and economic analysis of a SD with evacuated tube solar collector for drying Nile Tilapia slices. *Sci. Rep.* **15**, 9822 (2025).
44. Kidane, H., Farkas, I. & Buzás, J. Mathematical modelling of golden apple drying and performance evaluation of solar drying systems using energy and exergy approach. *Sci. Rep.* **15**, 7805 (2025).
45. Rahman, M. A., Hasnain, S. M. M., Paramasivam, P., Zairor, R. & Ayanie, A. G. Solar drying for domestic and industrial applications: A comprehensive review of innovations and efficiency enhancements. *Global Challenges* 2400301 (2025).
46. Ceballos, L. A. V. et al. Techno-economic and environmental assessment of a photovoltaic-thermal (PV-T) SD for habanero chili (*Capsicum chinense*): 4E (energy, economic, embodied and environmental) analysis. *Renew. Energy* **245**, 122758 (2025).
47. Jimoh, K. A., Hashim, N., Shamsudin, R., Man, H. C. & Jahari, M. Assessment of performance and quality indices of glutinous rice under different drying methods. *Sustain. Energy Technol. Assess.* **73**, 104161 (2025).
48. Hin, L., Buntong, B., Mean, C. M., Chhoem, C. & Prasad, P. V. V. Impacts of using SDs on socio-economic conditions of dried fish processors in Cambodia. *Sustainability* **16**, 2130 (2024).
49. Yazici, M. & Kose, R. Energy, exergy and economic investigation of novel hybrid dryer, indirect SD and traditional shade drying. *Therm. Sci. Eng. Prog.* <https://doi.org/10.1016/j.tsep.2024.102502> (2024).
50. Brahma, B., Shukla, A. K. & Baruah, D. C. Energy, exergy, economic and environmental analysis of phase change material based SD (PCMSD). *J. Energy Storage* **88**, 111490 (2024).
51. Zeng, Z. et al. Analysis of drying characteristic, effective moisture diffusivity and energy, exergy and environment performance indicators during thin layer drying of tea in a convective-hot air dryer. *Front Sustain. Food Syst.* **8**, 1371696 (2024).
52. Gupta, A., Das, B. & Mondol, J. D. Utilizing a novel method of sand-filled thermal energy storage system for performance enhancement in PVT SD. *Sol. Energy Mater. Sol. Cells* **283**, 113450 (2025).
53. Gupta, A., Borah, P. P., Das, B. & Mondal, J. D. Energy and exergy based performance evaluation of an innovative PV-assisted SD with and without modified absorber. *Sol. Energy* **272**, 112464 (2024).
54. Gupta, A. et al. Artificial neural networks based computational and experimental evaluation of thermal and drying performance of partially covered PVT SD. *Process Saf. Environ. Prot.* **183**, 1170–1185 (2024).
55. Gupta, A., Das, B., Biswas, A. & Mondol, J. D. Assessment of performance and quality parameters for drying neem leaves in photovoltaic-thermal SD. *Therm. Sci. Eng. Prog.* **43**, 101989 (2023).
56. Chandramohan, V. & Gilago, M. Performance evaluation of natural and forced convection indirect type SDs during drying ivy gourd: An experimental study. *Renew. Energy*. <https://doi.org/10.1016/j.renene.2021.11.038> (2021).

57. Mugi, V., Chandramohan, V. & Gilago, M. Energy and exergy investigation of indirect SD under natural and forced convection while drying muskmelon slices. *Energy Nexus*. <https://doi.org/10.1016/j.nexus.2022.100153> (2022).
58. Gilago, M. C., Mugi, V. R., Chandramohan, V. P. & Suresh, S. Evaluating the performance of an indirect SD and drying parameters of pineapple: Comparing natural and forced convection. *J. Therm. Anal. Calorim.* **148**, 3701–3709 (2023).
59. Chandramohan, V., Gilago, M. & Mugi, V. Evaluation of drying kinetics of carrot and thermal characteristics of natural and forced convection indirect SD. *Results Eng.* <https://doi.org/10.1016/j.rineng.2023.101196> (2023).
60. Natarajana, S. K. & Muthuvairavana, G. Experimental study on drying kinetics and thermal modeling of drying kohlrabi under different solar drying methods. *Therm. Sci. Eng. Prog.* <https://doi.org/10.1016/j.tsep.2023.102074> (2023).
61. Rani, P. & Tripathy, P. Drying characteristics, energetic and exergetic investigation during mixed-mode solar drying of pineapple slices at varied air mass flow rates. *Renew. Energy*. <https://doi.org/10.1016/j.renene.2020.11.107> (2020).
62. Ndukwu, M., Tagne, A. T., Marouani, M. E., Etala, H. D. T. & Simo-Tagne, M. Energy, environmental and economic analyses of an indirect cocoa bean SD: A comparison between natural and forced convections. *Renew. Energy*. <https://doi.org/10.1016/j.renene.2022.02.015> (2022).
63. Elkot, W. et al. Development, drying characteristics, and environmental analysis of a PV operated automatic SD for drying date. *Front Sustain. Food Syst.* <https://doi.org/10.3389/fsufs.2025.1531601> (2025).
64. Shimpy, Kumar, M. & Kumar, A. Designs performance and economic feasibility of domestic SDs. *Food Eng. Rev.* **15**, 156–186 (2022).
65. Elwakeel, A. E. et al. Development and techno-economic analysis of a tracked indirect forced SD integrated photovoltaic system for drying tomatoes. *Sustainability* **16**, 7008 (2024).
66. Tesfaye, A. & Habtu, N. G. Fabrication and performance evaluation of solar tunnel dryer for ginger drying. *Int. J. Photoenergy* **2022**, 1–13 (2022).
67. Mansour, N. E. et al. Automated vacuum drying kinetics, thermodynamics, and economic analysis of sage leaves. *Sci. Rep.* **15**, 18779 (2025).
68. El-Messery, T. et al. The mathematical modeling, diffusivity, energy, and enviro-economic analysis (MD3E) of an automatic SD for drying date fruits. *Sustainability*. <https://doi.org/10.3390/su16083506> (2024).
69. Karne, H., Bendre, A. & Singh, A. Mathematical modelling of a pilot scale biogas plant. *Mater. Today Proc.* (2023).
70. Aghbashlo, M., Kianmehr, M. H., Khani, S. & Ghasemi, M. Mathematical modelling of thin-layer drying of carrot. *Int. Agrophys.* **23**, 313–317 (2009).
71. Elwakeel, A. E. et al. Design and validation of a variable-rate control metering mechanism and smart monitoring system for a high-precision sugarcane transplanter. 1–20 (2023).
72. Elwakeel, A. E. et al. Design, construction and field testing of a manually feeding semiautomatic sugarcane dud chipper. *Sci. Rep.* **14**, 5373 (2024).
73. Yang, L. et al. A new automatic sugarcane seed cutting machine based on internet of things technology and RGB color sensor. *PLoS ONE* **19**, e0301294 (2024).
74. Elkhadraoui, A., Kooli, S., Hamdi, I. & Farhat, A. Experimental investigation and economic evaluation of a new mixed-mode solar greenhouse dryer for drying of red pepper and grape. *Renew. Energy* **77**, 1–8 (2015).
75. Mohammed, I. A. & Al Dulaimi, M. A. K. An economic analysis of the costs of producing tomato under greenhouse in Anbar governorate for the agricultural season 2019–2020. In *IOP Conference Series: Earth and Environmental Science* vol. 904 12061 (IOP Publishing, 2021).
76. Singh, P. & Gaur, M. K. Environmental and economic analysis of novel hybrid active greenhouse SD with evacuated tube solar collector. *Sustain. Energy Technol. Assess.* **47**, 101428 (2021).
77. Atheaya, D. Economics of Solar Drying. <https://doi.org/10.1007/978-981-10-3833-4> (2017).
78. Vijayan, S., Arjunan, T. V. & Kumar, A. Exergo-environmental analysis of an indirect forced convection SD for drying bitter gourd slices. *Renew. Energy* **146**, 2210–2223 (2020).
79. Prakash, O. & Kumar, A. Environmental analysis and mathematical modelling for tomato flakes drying in a modified greenhouse dryer under active mode. *Int. J. Food Eng.* **10**, 669–681 (2014).
80. Prakash, O. & Kumar, A. Solar greenhouse drying: A review. *Renew. Sustain. Energy Rev.* **29**, 905–910 (2014).
81. Baird, G., Alcorn, A. & Haslam, P. The energy embodied in building materials—updated New Zealand coefficients and their significance. *Trans. Inst. Prof. Eng. N. Z. Civ. Eng. Sect.* **24**, 46–54 (1997).
82. Jain, A., Sharma, M., Kumar, A., Sharma, A. & Palamanit, A. Computational fluid dynamics simulation and energy analysis of domestic direct-type multi-shelf SD. *J. Therm. Anal. Calorim.* **136**, 173–184 (2019).
83. Kumar, M., Sahdev, R. K., Tiwari, S., Manchanda, H. & Kumar, A. Enviro-economical feasibility of groundnut drying under greenhouse and indoor forced convection hot air dryers. *J. Stored Prod. Res.* **93**, 101848 (2021).
84. Ayyappan, S. Performance and CO₂ mitigation analysis of a solar greenhouse dryer for coconut drying. *Energy Environ.* **29**, 1482–1494 (2018).
85. Tiwari, S. et al. Environmental and economic sustainability of PVT drying system: A heat transfer approach. *Environ. Prog. Sustain. Energy* **40**, e13535 (2021).
86. Selimefendigil, F., Şirin, C., Ghachem, K. & Kolsi, L. Exergy and environmental analysis of an active greenhouse dryer with Al₂O₃ nano-embedded latent heat thermal storage system: An experimental study. *Appl. Therm. Eng.* **217**, 119167 (2022).
87. Barnwal, P. & Tiwari, G. N. Life cycle energy metrics and CO₂ credit analysis of a hybrid photovoltaic/thermal greenhouse dryer. *Int. J. Low Carbon Technol.* **3**, 203–220 (2008).
88. El Magd, W. A. & Elwakeel, A. E. Study on some properties of tomato fruits for natural sun drying. *J. Soil Sci. Agric. Eng.* **12**, 763–767 (2021).
89. Djebli, A., Hanini, S., Badaoui, O. & Boumahdi, M. A new approach to the thermodynamics study of drying tomatoes in mixed SD. *Sol. Energy* **193**, 164–174 (2019).
90. Zambare, A. & Kulkarni, D. Experimental investigation on drying of tomato slices. *J. Pharmacogn. Phytochem.* <https://doi.org/10.22271/phyto.2023.v12.i6a.14761> (2023).
91. Yanniotis, S., Xanthopoulos, G. & Talaiporou, E. Influence of salting on drying kinetics and water diffusivity of tomato halves. *Int. J. Food Prop.* **15**, 847–863 (2012).
92. Ghaly, A. & El-Hana, N. International journal of food engineering effect of osmotic pre-treatment on the air-drying behavior and quality of plum tomato pieces (2011).
93. Ringeisen, B., Barrett, D. & Stroewe, P. Concentrated solar drying of tomatoes. *Energy Sustain. Dev.* **19**, 47–55 (2014).
94. Djebli, A., Hanini, S., Badaoui, O. & Boumahdi, M. A new approach to the thermodynamics study of drying tomatoes in mixed SD. *Sol. Energy* <https://doi.org/10.1016/j.solener.2019.09.057> (2019).
95. Hamdi, I., Agrebi, S., Elkhadraoui, A., Chargui, R. & Kooli, S. Qualitative, energy and economic analysis of forced convective solar drying of tomatoes slices. *Sol. Energy*. <https://doi.org/10.1016/j.solener.2023.04.021> (2023).
96. Doymaz, İ. Evaluation of some thin-layer drying models of persimmon slices (*Diospyros kaki* L.). *Energy Convers. Manag.* **56**, 199–205 (2012).
97. Kaleta, A., Górnicki, K., Winiczenko, R. & Chojnacka, A. Evaluation of drying models of apple (var. Ligol) dried in a fluidized bed dryer. *Energy Convers. Manag.* **67**, 179–185 (2013).
98. Meziiane, S. Drying kinetics of olive pomace in a fluidized bed dryer. *Energy Convers. Manag.* **52**, 1644–1649 (2011).

99. Nassef, A. M., Rahman, S. M. A., Rezk, H. & Said, Z. ANFIS-based modelling and optimal operating parameter determination to enhance cocoa beans drying-rate. *IEEE Access* **8**, 45964–45973 (2020).
100. Etim, P. J., Eke, A. B. & Simonyan, K. J. Design and development of an active indirect SD for cooking banana. **8** (2020).
101. Hossain, M. A., Amer, B. M. A. & Gottschalk, K. Hybrid SD for quality dried tomato. *Dry. Technol.* **26**, 1591–1601 (2008).
102. Song, X., Zhang, M. & Mujumdar, A. S. Effect of vacuum-microwave predrying on quality of vacuum-fried potato chips. *Dry. Technol.* **25**, 2021–2026 (2007).
103. Farag, S.E.-S., Hassan, S. R., Younes, O. S. & Taha, S. A. Methods of drying of tomato slices and the effect of the using of its powder on the production and characteristics of extruded snacks. *Misr J. Agric. Eng.* **33**, 1537–1558 (2016).
104. Téllez, M. C., Figueroa, I. P., Téllez, B. C., Vidana, E. C. L. & Ortiz, A. L. Solar drying of stevia (*Rebaudiana bertonii*) leaves using direct and indirect technologies. *Sol. Energy* **159**, 898–907 (2018).
105. Sacilik, K., Keskin, R. & Elicin, A. K. Mathematical modelling of solar tunnel drying of thin layer organic tomato. *J Food Eng* **73**, 231–238 (2006).
106. Ismail, O. & Akyol, E. Open-air sun drying: The effect of pretreatment on drying kinetic of cherry tomato. *Sigma J. Eng. Nat. Sci.* **34**, 141–151 (2016).
107. Dissa, A. O., Desmorieux, H., Bathiebo, J. & Kouliadi, J. A comparative study of direct and indirect solar drying of mango. *Global J. Pure Appl. Sci.* **17**, 273–294 (2011).
108. Navale, S. R., Harpale, V. M. & Mohite, K. C. Comparative study of open sun and cabinet solar drying for fenugreek leaves. *Int. J. Renew. Energy Technol. Res.* **4**, 1–9 (2015).
109. Stephen, T. K. University of Nairobi School of Engineering 2009 (2014).
110. Babar, O. A., Tarafdar, A., Malakar, S., Arora, V. K. & Nema, P. K. Design and performance evaluation of a passive flat plate collector SD for agricultural products. *J. Food Process. Eng.* 1–13 (2020).
111. Onwude, D. I., Hashim, N., Janius, R. B., Nawi, N. M. & Abdan, K. Modeling the thin-layer drying of fruits and vegetables: A review. *Compr. Rev. Food Sci. Food Saf.* **15**, 599–618 (2016).
112. He, C. et al. Drying behavior and kinetics of drying process of plant-based enteric hard capsules. *Pharmaceutics* **13**, 335 (2021).
113. Bispo, J. A. C., Bonafe, C. F. S., Santana, K. M. O. V. & Santos, E. C. A. A comparison of drying kinetics based on the degree of hydration and moisture ratio. *LWT-Food Sci. Technol.* **60**, 192–198 (2015).
114. Heredia, A., Barrera, C. & Andrés, A. Drying of cherry tomato by a combination of different dehydration techniques. Comparison of kinetics and other related properties. *J. Food Eng.* **80**, 111–118 (2007).
115. Xanthopoulos, G., Yanniotis, S. & Talaiporou, E. Influence of salting on drying kinetics and water diffusivity of tomato halves. *Int. J. Food Prop.* **15**, 847–863 (2012).
116. Azumah, L. C., Abu, M., Kaburi, S. A. & Lamptey, F. P. Effect of pre-drying treatments on the quality of solar-dehydrated tomato (*Lycopersicon esculentum* L.) fruits. *Appl. Food Res.* <https://doi.org/10.1016/j.afres.2024.100422> (2024).
117. Lingayat, A. B., Vp, C., Raju, V. R. K. & Sivan, S. Drying kinetics of tomato (*Solanum lycopersicum*) and Brinjal (*Solanum melongena*) using an indirect type SD and performance parameters of dryer. *Heat Mass Transf.* **57**, 853–872 (2020).
118. Dufera, L. T., Hofacker, W., Esper, A. & Hensel, O. Experimental evaluation of drying kinetics of tomato (*Lycopersicon Esculentum* L.) slices in twin layer solar tunnel dryer. *Energy Sustain. Dev.* **61**, 241–250 (2021).
119. Akhijani, H., Arabhosseini, A. & Kianmehr, M. Effective moisture diffusivity during hot air solar drying of tomato slices. *Res. Agric. Eng.* **62**, 15–23 (2016).
120. Nwakuba, N., Chukwuezie, O., Asoegwu, S., Nwandikom, G. & Okereke, N. Energy requirements and effective moisture diffusivity of tomato slices in a hybrid convective dryer. **1**. <https://doi.org/10.13031/AIM.201800038> (2018).
121. Olimat, A. International Journal of Renewable Energy Development (2020).
122. Nettiari, C. et al. Design and performance evaluation of an innovative medium-scale SD with heat recovery based-latent heat storage: Experimental and mathematical analysis of tomato drying. *J. Energy Storage.* <https://doi.org/10.1016/j.est.2024.111559> (2024).
123. Midilli, A. & Kucuk, H. Mathematical modeling of thin layer drying of pistachio by using solar energy. *Energy Convers. Manag.* **44**, 1111–1122 (2003).
124. Akpinar, E. K. & Bicer, Y. Mathematical modeling and experimental study on thin layer drying of strawberry. *Int. J. Food Eng.* **2** (2006).
125. Akpinar, E. K., Bicer, Y. & Cetinkaya, F. Modelling of thin layer drying of parsley leaves in a convective dryer and under open sun. *J. Food Eng.* **75**, 308–315 (2006).
126. Sharshir, S. W., Joseph, A., Elsayad, M. M., Hamed, M. H. & Kandeal, A. W. Thermo-enviroeconomic assessment of a SD of two various commodities. *Energy* **295**, 130952 (2024).
127. Andharia, J. K., Markam, B., Patel, J. & Maiti, S. Study of a mixed-mode SD integrated with photovoltaic powered dehumidifier. *Sol. Energy* **273**, 112505 (2024).
128. Kusun, B. et al. Experimental and numerical analysis of a grooved hybrid photovoltaic-thermal solar drying system. *Appl. Therm. Eng.* <https://doi.org/10.1016/j.applthermaleng.2022.119288> (2022).
129. Aktas, M. & Arslan, E. 4E analysis of infrared-convective dryer powered solar photovoltaic thermal collector. *Sol. Energy* **208**, 46–57 (2020).
130. Cankurtaran, E. & Atalay, H. Energy, exergy, exergoeconomic and exergo-environmental analyses of a large scale SD with PCM energy storage medium. *Energy* <https://doi.org/10.1016/j.energy.2020.119221> (2020).
131. Zeeshan, M. et al. Novel design and performance evaluation of an indirectly forced convection desiccant integrated SD for drying tomatoes in Pakistan. *Heliyon* **10**, e29284 (2024).
132. Sharma, M., Atheaya, D. & Kumar, A. Performance evaluation of indirect type domestic hybrid SD for tomato drying: Thermal, embodied, economical and quality analysis. *Ther. Sci. Eng. Prog.* **42**, 101882 (2023).

Acknowledgements

The authors would like to acknowledge Deanship of Graduate Studies and Scientific Research, Taif University for funding this work.

Author contributions

Conceptualization, A.E.E., methodology, A.E.E., G.A., M.M.A., software, A.E.E., M.M.A., validation, A.E.E., formal analysis, A.E.E., G.A., and M.M.A., K.A.M., investigation, A.E.E., G.A., A.Z.E., resources, A.E.E., M.S.A., A.F.A., data curation, A.E.E., and M.M.A., K.A.M., Writing—original draft, A.E.E., writing—review and editing, A.E.E., G.A., A.Z.E., visualization, A.E.E., supervision, A.E.E., project administration, A.E.E., funding acquisition, A.E.E., M.S.A., All authors have read and agreed to the published version of the manuscript.

Funding

This research was funded by the Deanship of Graduate Studies and Scientific Research, Taif University.

Declarations

Competing interests

The authors declare no competing interests.

Additional information

Correspondence and requests for materials should be addressed to A.E.E. or G.A.

Reprints and permissions information is available at www.nature.com/reprints.

Publisher's note Springer Nature remains neutral with regard to jurisdictional claims in published maps and institutional affiliations.

Open Access This article is licensed under a Creative Commons Attribution-NonCommercial-NoDerivatives 4.0 International License, which permits any non-commercial use, sharing, distribution and reproduction in any medium or format, as long as you give appropriate credit to the original author(s) and the source, provide a link to the Creative Commons licence, and indicate if you modified the licensed material. You do not have permission under this licence to share adapted material derived from this article or parts of it. The images or other third party material in this article are included in the article's Creative Commons licence, unless indicated otherwise in a credit line to the material. If material is not included in the article's Creative Commons licence and your intended use is not permitted by statutory regulation or exceeds the permitted use, you will need to obtain permission directly from the copyright holder. To view a copy of this licence, visit <http://creativecommons.org/licenses/by-nc-nd/4.0/>.

© The Author(s) 2025